XA9437028

International Atomic Energy Agency

INDC(BLR)-001
Distr.: L

INDC INTERNATIONAL NUCLEAR DATA COMMITTEE

EVALUATED NEUTRON DATA FOR URANIUM-233

L.A. Bakhanovich, A.B. Klepatskij, V.M. Maslov, G.B. Morogovskij,
Yu.V. Porodzinskij, E.Sh. Sukhovitskij

Department of Scientific and Technical Information
Nuclear Power Institute, Byelorussian SSR Academy of Sciences
Minsk 1991

Responsible Officer: A.B. Klepatskij
Editor and proof-reader: L.M. Ivanova

Translated by Dr. A. Lorenz for the IAEA
from Russian preprint IYaEh-2(25) (1992)

December 1993

INDC(BLR)-001
Distr.: L

EVALUATED NEUTRON DATA FOR URANIUM-233

L.A. Bakhanovich, A.B. Klepatskij, V.M. Maslov, G.B. Morogovskij,
Yu.V. Porodzinskij, E.Sh. Sukhovitskij

Department of Scientific and Technical Information
Nuclear Power Institute, Byelorussian SSR Academy of Sciences
Minsk 1991

Responsible Officer: A.B. Klepatskij
Editor and proof-reader: L.M. Ivanova

Translated by Dr. A. Lorenz for the IAEA
from Russian preprint IYaEh-2(25) (1992)

December 1993

EVALUATED NEUTRON DATA FOR URANIUM-233

L.A. Bakhanovich, A.B. Klepatskij, V.M. Maslov,
G.B. Morogovskij, Yu. V. Porodzinskij, E. Sh. Sukhovitskij

ABSTRACT

The evaluation of the properties of the interaction of neutrons with the 233U nucleus prepared for the neutron data evaluated file BROND is presented. Existing neutron interaction data is supplemented by evaluations of experimental data. Other types of nuclear data and other energy ranges are investigated by means of theoretical calculations and systematics. The evaluated data obtained in this work are compared with experimental data and evaluations prepared by other authors.

INTRODUCTION

Recently, interest in the development of an advanced design for the nuclear power sector using a mixed thorium and uranium fuel cycle has increased significantly. One important advantage of a thorium fuel cycle is that the resulting radioactive waste would not need to be confined for such long periods of time. However, development of the thorium cycle has been held up mainly by the high cost of producing the highly enriched uranium ^{233}U which it requires.

It would appear that by going over to using the ^{233}U accumulated as a result of loading thorium in the blankets of fast reactors, we can overcome the difficulties associated with the use of thorium [1, 2]. However, effective neutron-physics studies on such reactors will require a knowledge of the nuclear data for all nuclides associated with the thorium fuel cycle, which are not at present available in our national library of evaluated neutron data.

The present evaluation of a complete file of neutron data for ^{233}U is part of the work aimed at establishing neutron data files for all the nuclides of importance in the thorium cycle. The ^{233}U nuclide is produced by the following reaction in the neutron flux of a reactor:

$$^{232}Th(n,\gamma)\ ^{233}Th \xrightarrow[(22,3\pm0,21)\ min]{\beta^-} {}^{233}Pa \xrightarrow[(27,0\pm0,1)\ days]{\beta^-} {}^{233}U.$$

The half-life of ^{233}U is (1.592 ± 0.002) x 10^5 years for α-decay and (1.2 ± 0.3) x 10^{17} years for spontaneous fission [3].

The table below lists the energy Q values and thresholds T [4, 5] of various neutron reactions involving the ^{233}U nucleus, which are linked by the relationship

$$T = \frac{M_n + M_{233}}{M_{233}} \cdot (-Q) = \frac{1{,}0086652 + 233{,}039654}{233{,}039654} \cdot (-Q) = 1{,}0043283 \cdot (-Q).$$

ENERGY Q VALUES AND THRESHOLD T VALUES FOR NEUTRON REACTIONS INVOLVING THE 233U NUCLIDE, IN MEV

Reaction	Q	T	Reaction	Q	T
(n,γ)		-6.841	(n,nd)	-9.638	9.68
(n,2n)	-5.744	5.769	(n,t)	-3.385	3.40
(n,3n)	-13.008	13.064	(n,nt)	-10.206	10.25
(n,4n)	-18.906	18.988	(n,^{3}He)	-3.754	3.77
(n,p)	-0.213	0.214	(n,n^{3}He)	-8.882	8.92
(n,np)	-6.307	6.334	(n,^{4}He)		-11.70
(n,d)	-4.082	4.100	(n,n^{4}He)		-4.91

1. EVALUATED NEUTRON DATA FOR ^{233}U IN THE RESOLVED RESONANCE REGION (10^{-5}-100 eV)

For the purpose of our evaluation, the resolved resonance region was divided into two parts: the thermal range (10^{-5}-1 eV), where the cross- sections can be considered to have practically no dependence on the temperature of the sample and therefore can be presented point-wise; and the parametrized resonance range (1-100 eV), in which the cross-sections can be obtained from evaluated parameters.

1.1. The thermal energy range (10-5-1 eV)

The evaluated cross-sections in the thermal range are quoted point- wise, as the use of resonance formulae for analysis in this

range is cumbersome owing to the necessity of selecting positions and values for the negative resonance parameters (there may be more than one), and the great sensitivity of cross-sections in the thermal range to changes in the resolved resonance parameters. Also, a better description and harmonization of the whole set of experi data can be obtained from a point-wise presentation of the cross-sections.

Preliminary analysis of the available information led to the following sets of experimental data:

(1) For σ_t - Kolar et al. [6], Brooks et al. [7], Vertebnyj et al. [11], Harvey et al. [12], Block et al. [13], Muether et al. [14], Pattenden et al. [15];

(2) For σ_f - Cao et al. [16], Deruytter et al. [17], Sanders et al. [18], Pshenichnyj et al. [9], Weston et al. [19, 20], Moore et al. [11];

(3) For σ_γ - Weston et al. [19, 20];

(4) For σ_n - Vertebnyj et al. [8], Olekca [21];

(5) For η - Brooks et al. [7], Pshenichnyj et al. 49], Weston et al. [20], Sanders et al. [22], Smith et al. [23, 24], Magleby et al. [25], Pavlesky et al. [26].

The selection was based on fairly detailed experimental information, in particular on a knowledge of the authors' normalization (which is essential) for σ_f, σ_γ and η, and also the absence of any inconsistencies between the different sets of data.

The normalizing values of the data at thermal are taken from Ref. [27]:

$\sigma_t = 587.60 \times 10^{-28}\ m^2$, $\sigma_n = 12.60 \times 10^{-28} m^2$,

$\sigma_f = 529.60 \times 10^{-28}\ m^2$, $\eta = 2.2960$,

$\sigma_\gamma = 45.40 \times 10^{-28}\ m^2$, $\upsilon_t = 2.4928$.

The experimental data for σ_f, σ_γ and η were renormalized to new data values at 0.0253 eV on the basis of information about previous normalization given in the relevant papers, and the σ_t data of those authors who indicated their normalization were renormalized in exactly the same way. Where there was no information about normalization procedures in total cross-section

experiments, or where it seemed unreliable, irrespective of the type of data, the normalization was calculated by the familiar method of Block and co-workers [13], if measurements had been made in the thermal region and there were enough of them to make the calculation possible. In the remaining cases normalization was performed on the basis of integrals to already normalized data sets which appeared to be more reliable than others.

Subsequently, statistical weights were assigned to all the selected data sets on the basis of the available experimental information and an intercomparison of the detailed cross-section curves. The PREDA-M program - a modification of the PREDA program described in Ref. [28] - was used to process the experimental values for σ_t, σ_f, σ_γ and η, and the processing procedure was run separately for each type of data, taking their statistical weights into consideration. Note that the values of the scattering cross-section quoted in Refs [8, 21] are not in agreement with the value of σ_n^{2200} which was used in our present work, besides which the measurements started only from υ at 0.1 eV. The behavior of the scattering cross-section was derived from the resolved resonance parameters on the basis of a value of $\sigma_n^{2200} = 12.6 \times 10^{-28}\,m^2$, and taking the radius of the potential scattering to be equal to 9.5784 fm.

The evaluated cross-section values for σ_t, σ_f and σ_γ as well as for the quantity η are not entirely consistent, and there are distortions in the $\alpha(E)$ curve obtained from evaluations of σ_f and σ_γ. All of this suggests that the initial experimental values must have been of poor quality. Great care is called for in handling Weston's σ_γ data [19, 20], which were calculated on the basis of σ_γ measurements that relied on the σ_t data from Refs [11, 15] and on Weston's own σ_f values [19, 21]. From the diagram reproduced in Ref. [19] it can be seen that in the energy interval 0.07-0.35 eV the total cross-section obtained by the authors on the basis of their σ_f and σ_γ data and Drake's σ_n values [29] is systematically higher than Moore's σ_t values [11] which were used to calculate the values of σ_γ. To all appearances, therefore, the σ_γ cross-sections in Ref. [19] and consequently in the independent evaluation of σ_γ were too high, which in turn meant introducing a discrepancy in the

quantities η and α. Given these circumstances, calculated values of the cross-sections σ_t, σ_f, σ_n and the generally accepted value of ν_t were used as reference values in deriving the complete set of evaluated nuclear data. Results for $\eta(E)$ obtained in an independent operation, and also $\eta(E)$ and $\alpha(E)$ results calculated from evaluated cross-section values, were used to monitor the quality of the nuclear data evaluation. The behavior of the cross-sections in the low-energy region (from thermal to 10^{-5} eV), where no reliable experimental information was available, was derived from an extrapolation of evaluated data. The g-factor values obtained were the following: $g_a = 0.9980$, $g_f = 0.9955$, and $g_p = 1.0273$.

When the calculated values for σ_t, σ_f and σ_γ were analyzed, it became apparent that there was a certain discrepancy in the behavior of the curves in the energy interval 0.35-0.55 eV, the cause of which is still unknown. It seems unlikely that this distortion would arise in the mathematical treatment of the experimental data or that it could be a random phenomenon. Each set of data for σ_t and σ_f which overlapped the aforementioned range was processed separately: Refs [7-12, 15] for σ_t and [11, 16-20] for σ_f. The distortion in the behavior of the cross-section proved to be present in almost all sets. Exceptions were found in the σ_t measurements of Ref. [15] and in the σ_f measurements of Refs [16, 18], but the experimental fission cross-section values in [16] show a wide scatter in this region, and Ref. [18] contains few data. If we assume that the distortion is due to the presence of impurity in the samples, then, bearing in mind that the effect appears both in the total cross-section and in the fission cross-section, and considering also the size of the distortion, the logical conclusion would seem to be that there is a significant ^{237}Np or ^{241}Am impurity present. However, according to the authors' data on the isotopic composition of their samples there are no such impurities: the samples are composed entirely of uranium mixtures, and in Weston's experimentalments [19, 20] consist of 99.99% ^{233}U. Thus, we can only assume that there is a weak resonance of ^{233}U at an energy around 0.49 eV. A definitive answer to the question whether such a resonance exists may emerge from polarized neutron measurements similar to those in Moore's experimentalment [30].

Numerical values of the evaluated cross-sections in the energy interval 10^{-5}-1 eV are contained in the ^{233}U file.

1.2. Parametrization of cross-sections in the resolved resonance region (1-100 eV)

To evaluate ^{233}U neutron cross-sections in the resolved resonance region and derive recommended parameter values is quite a complicated task. The fact is that the quality of the available experimental measurements of σ_t, σ_f and σ_γ is far from satisfactory; the resonances are located quite close to each other, and this fact, together with the fairly large total width ($< D > \approx 0.7$ eV, $< \Gamma >/< D > \approx 0.6$) complicates parametrization because of the appreciable interference between levels. The situation in the resolved resonance region for ^{233}U is very similar to the one which existed up until 1978 in the same region for ^{235}U. The appearance at that time of Moore's work [30], brought about a marked improvement in the quality of the ^{235}U recommended resonance parameters thanks to genuinely new information about the number of resonances and their spins. To solve the problem of the status of "artificial" resonances [31] and of the levels missed in experiments, measurements should be made analogous to those in Ref. [30].

A survey of existing cross-section measurements has shown that the following data sets can be used for parametrization:

(1) For σ_t - Kolar et al. [6], Moore et al. [11], Pattenden et al. [15];

(2) For σ_f - Moore et al. [11], Cao et al. [16], Deruytter et al. [17], Weston et al. [20], Blons et al. [32];

(3) For σ_γ - Weston et al. [20].

After detailed analysis of the information available on the measurements mentioned above, the following selections were made for further work: for σ_t - [6]; for σ_f - [17, 32]; for σ_γ - [20]. The remaining experimental data were not used because the energy resolution was substantially worse than in the references which were selected.

In parametrization, especially when three types of cross-section are being considered simultaneously, as in the present case, it is very important that the energy scales used in different experiments should be the same. Any inconsistency in the scales may lead to the appearance of abnormal or even non-physical parameter values. In our present work the resonance energies from Ref. [31] have been used, and appropriate energy adjustments were made in experimental data sets which did not coincide with this scale. Thirteen fairly pronounced and well-resolved resonances were selected as our basic resonances in the energy interval 2-100 eV.

Statistical weights based on available information about the experimental conditions and the behavior of the cross-sections were assigned to all the data sets used. Furthermore, even at the stage of preliminary analysis there were grounds to suppose that we would find poor agreement between the experimental data on different types of cross-sections, and this was in fact confirmed later on. Thus, the weight for a particular experimentalment was a numerical expression reflecting the quality of the cross-section involved in parametrization. As was to be expected, the lowest weight was assigned to the radiative capture cross-section data from Ref. [20].

Average values of the cross-sections from different authors, cited in Ref. [17], were used to normalize the fission and radiative capture cross- sections. The fact that Deruytter's fission cross-section had already been renormalized to the new value of σ_f^{2200} [27] was taken into account here. The radiative capture cross-section from Ref. [20] was renormalized, just as it would have been necessary to renormalize the fission cross-section from Ref. [20] in order to preserve the value of α.

The parameters in the energy interval 1-100 eV were calculated by the Breit-Wigner and Adler-Adler formalism, and the parametrization method used was that in which the parameters G and H are matched. The quality of the parametrization for each formalism was assessed in the same way as in Ref. [33]. In the energy interval under consideration there are 149 resonances, although the file records parameter values for 178. For two

resonances below 1 eV (E_r = -3 eV and E_r = 0.17 eV) the Breit-Wigner and Adler-Adler parameters were derived separately through an evaluation of neutron data in the thermal range. The parameters of 27 resonances above 100 eV were taken from Ref. [34]. Parametrization in the 1-100 eV interval took into account the contribution of these additional 29 resonances to the cross-sections.

The work carried out in the manner described above yielded two sets of parameters derived from the Breit-Wigner and Adler-Adler formalisms, each of which provided an optimal description of the whole body of initial experimental data within the framework of the corresponding formalism when the weights assigned to them were taken into account. A "flat spectrum" was then calculated for each set of parameters with due allowance for the conditions indicated in Ref. [35]. It became clear that this improved the description of the experiments by 25-30%. The "flat spectrum" for each set of parameters contains about 300 points; this is quite acceptable, especially if one considers that a third of the file relates to the interval 1-15 eV, and that 40 points fall into the range 1-5 eV. The aforementioned fact results from the poor agreement of the experimental data, which is very noticeable for example in the 1.78 and 2.29 eV resonances, which have large errors in the total cross-section peaks due to the relatively great thickness of the sample used in Ref. [6].

The evaluation of parametrization quality showed that the best description of the whole body of initial experimental cross-sections is given by self-consistent Adler parameters with a "flat spectrum", and for this reason they were included in the evaluated data file. However, it should be noted that a third of the parametrized resonances have zero interference for all three types of cross-section, which means that they are of the Breit-Wigner type. If we compare the accuracy of the description of the experiments given by the two parameter systems, ignoring the "flat spectrum", then we may conclude that, on the whole, the Breit-Wigner parameters reproduce the initial cross-sections somewhat better (about 4-5% better). This is because of the low quality of the experimental data and the long-range interaction

of the Adler interference parameters, which is very hard to assess.

The following limitations were selected for the parameters obtained by parametrization using the two formalisms: total width $\Gamma \leq 1.6$ eV, and radiation width $0.02 \leq \Gamma_\gamma \leq 0.06$ eV. It turned out that, for the Breit-Wigner parameters, 19 values of Γ and 53 values of Γ_γ have the maximum permissible values; for the Adler parameters there are 13 and 51 respectively. Average resonance parameters obtained from the two sets of parameters - both for all resonances up to 100 eV, and leaving out resonances which have the maximum permissible values of Γ and Γ_γ - are listed in Table 1.1.

Table 1.1
Average resonance parameters

No.of reso-nances	$\langle\Gamma^o_n\rangle$ eV	υ for Γ_f	$\langle\Gamma_\gamma\rangle$ eV	υ for Γ_f	Γ_γ eV	υ for Γ_γ	S_o $(eV)^{-1/2}$
150	1.304×10^{-4}	1.41	0.558	2.41	0.0363	14.21	0.973×10^{-4}
97	1.601×10^{-4}	1.92	0.344	2.98	0.0395	33.04	1.195×10^{-4}
150	1.290×10^{-4}	1.37	0.516	2.29	0.0353	14.17	0.963×10^{-4}
95	1.664×10^{-4}	2.07	0.364	2.48	0.0384	34.59	1.243×10^{-4}

Table 1.2
Group-averaged cross-sections for ^{233}U, 10^{-28} m^2

ΔE, eV	σ_t	σ_n	σ_f	σ_γ
1.0-2.15	429.94	10.45	359.11	60.39
2.15-4.65	186.41	11.87	125.53	49.01
4.65-10.0	130.05	10.69	101.23	18.12
10.0-21.5	143.41	11.14	112.81	19.47
21.5-46.5	90.0	12.14	70.65	7.22
46.5-100.0	57.71	11.90	39.09	6.72

The first two lines of the table refer to the Breit-Wigner parameter set, the third and fourth to the Adler set.

Group-averaged cross-section values derived from the resonance parameters with the addition of the "flat spectrum" are listed in Table 1.2.

Let us note in conclusion that it will be possible to improve the reliability of the resonance parameters and associated quantities if new experimental measurements are made for all types of cross-sections in the resolved resonance region.

2. NEUTRON CROSS-SECTIONS IN THE UNRESOLVED RESONANCE ENERGY RANGE 0.1-40.35 keV

The evaluation of the ^{233}U unresolved resonance range in this evaluation is limited to the energy range of 0.1-40.35 keV. The lower boundary is defined by the extent of the experimentally resolved resonance range, and the upper boundary is related to the opening of an inelastic scattering channel and the lack of information on the strength function S_2. The resonance self-shielding factors for energies in the range defined by the upper limit are equal to the unit to a high degree of accuracy, which is indicative an overlapping of resonances and the correct choice of the boundary between regions of unresolved resonances and smooth cross-sections of the ^{233}U nucleus.

This evaluation takes account of the possibility of splitting the ^{234}U compound nucleus subsequent to the preliminary release of a γ-quantum. This process significantly reduces the radiative capture cross-section of the nucleus in question and is treated as fission in the experiments. Study of the interaction process of the neutron with the ^{233}U nucleus is limited by the consideration of the s- and p-waves.

2.1. Experimental data used to evaluate average interval cross-sections in the unresolved resonance range.

Cross-sections in the unresolved resonance range have a complex structure, thus data with a good resolution should be

used to estimate the group-averaged cross-sections. Time-of-flight measurements meet these requirements. Measurements at individual energy points are mainly averages over intervals, and the averaging is carried out with an unknown weighting function, thus the point data can be used only to verify the consistency of the estimate.

The experimental total cross-sections in papers by Moore [11], Fulwood [36], Kolar [6], Pattenden [15] and Poenitz [37] were averaged over standard energy intervals. The latter data were averaged to an energy of 100 keV, which is necessary for a reliable determination of the strength function S_1. The averaging results are shown in Fig. 2.1.

The figure shows significant correlations in the structure of cross-sections found by various different authors, but the total cross-sections [11], measured within a narrow energy range, lie much higher than the other data and these cross-sections are hard to describe with the reasonable values of the strength function S_0 and the potential scattering radius. The data in Ref. [36] do not include information on errors, and they are lower than all of the low-energy cross-sections. The data in Ref. [6] are a little higher than the data in Ref. [15], but they correlate well with each other, and at energies of over 0.4 keV they also agree on an absolute value. Clearly, the large average cross-sections in Kolar's paper are due to the energy resolution being better than that in Pattenden's paper.

On obtaining average interval cross-sections, only the data from Kolar, Pattenden and Poenitz's papers were used (at energies above 40 keV). The average interval total cross-sections obtained are given in Table 2.1.

The data on the ^{233}U fission cross-section in the range of unresolved resonances are not in themselves absolute and are normalized to the thermal cross-section or resonance interval. More accurate resonance fission integrals were measured in Deruytter's paper [17]:

$$I_1 = \int_{0.75\,eV}^{0.1\,eV} \sigma_f \, dE = (1170.8 \pm 5.9) \cdot 10^{-28} m^2 \cdot eV ; \quad I_2 = \int_{8.1\,eV}^{17.6\,eV} \sigma_f \, dE = (968.7 \pm 10.0) \cdot 10^{-28} m^2 eV$$

These integrals are related to the value of the thermal fission cross-section σ_{fo} = (529.6 ± 1.35) $\cdot 10^{28}$ m^2 used in the measurement. As shown in Section 1, this paper takes that value of the thermal fission cross-section. Integrals I_1 and I_2 are therefore taken to be 1161.8 and 961.26 respectively.

The cross-sections measured in papers by Blons [38], Gwin [39], Weston [20], Mostovaya [40] and Bergman [41] were used as source data to evaluate the fission cross-section . In the unresolved resonance range, other time-of-flight measurements were also taken into account. These are in papers by Moore [11], Bergen [42], Cao [16] and Albert [43]. However, careful consideration of the integrals obtained from these papers shows that in the different energy groups they require significantly different renormalization to correspond with the given integrals, which means that these data cannot be used in broad energy intervals.

The data selected are normalized standardized in a uniform manner to values taken at thermal and resonance integrals, and when necessary renormalized to the new value of the standard $^{10}B(n,\alpha)$ cross-section . The data obtained are shown in Fig. 2.2.

Some of the papers used, including Gwin, Bergman and Mostovaya, present the data in broader intervals than those given in this paper, initially the average cross-sections were obtained for these intervals considering all available data and their error; the data were then broken down into more detailed group structure in accordance with the data from papers by Blons and Weston. This explains the fact that in some energy intervals the average fission cross-section lies beyond the boundaries of all of the values considered by these authors. The group-averaged fission cross-sections thus obtained are given in Table 2.2.

The value of α for ^{233}U in the unresolved resonance range is presented in the only paper which reports on simultaneous measurement of the cross-sections σ_f and σ_γ in the range up to 2 keV [20]. The mean cross-section ratios $\langle\sigma_\gamma\rangle/\langle\sigma_f\rangle$ obtained from this paper in the given energy intervals are shown in Table 2.3.

2.2. Energy dependence of average resonance parameters

The average cross-sections in the unresolved resonance range were calculated from the average resonance parameters using the conventional method.

The average distances between levels $\langle D_J \rangle$ with spin J were determined from values of $\langle D_{ev} \rangle$ in the resolved resonance energy range using the level density from the superfluid nucleus model with allowance for collective modes [44, 45]. The average neutron widths were calculated from the strength functions S_ℓ:

$$\langle \Gamma_n \rangle^\ell_J = S_\ell \langle D \rangle_J E^{1/2} P_\ell$$

where P_ℓ are the transmission coefficients of the partial wave ℓ, calculated using the black nucleus model.

The fission widths were presented in the single-hump barrier approximation using the Hill-Wheeler model:

$$\langle \Gamma_f \rangle_{J\pi} = \frac{\langle D \rangle_J}{2\pi} \cdot \sum_i \frac{1}{1 + \exp\left[\frac{2\pi (E_{fi}^{J\pi} - E)}{\hbar\omega}\right]},$$

where $E_{fi}^{J\pi}$ are the fission barrier thresholds for specified J^π, whose relative position was selected mainly according to the scheme presented by Lynn [46].

The energy dependence of radiation widths was determined from the γ-quantum cascade emission model with allowance for the possibility of fission occurring subsequent to the gamma ray emission (reaction $(n,\gamma f)$). Thus, in addition to the $\langle \Gamma_\gamma \rangle^J$, and the $\langle \Gamma_{\gamma f} \rangle^J$ widths, which according to the assumptions has the same distribution as the radiation width, was also calculated. The dipole resonance parameters required to determine the energy dependence of the probability of γ-quantum emission, were taken from Ref. [46].

2.3. Evaluation of neutron cross-sections and average resonance parameters in the unresolved resonance range.

The first step in evaluating the average resonance parameters was the evaluation of the average optical parameters: the potential scattering radius R_0 and the power functions S_0 and

S_1 which were found by fitting the smooth theoretical curve to the set of group-averaged total cross-sections (Table 2.1). These parameters, which give a general description of the average total cross-sections are: $R_0 = 9.6 \times 10^{13}$ cm;

$S_0 = 0.99 \times 10^{-4}$ $(eV)^{-1/2}$;

$S_1 = 1.54 \times 10^{-4}$ $(eV)^{-1/2}$.

The corresponding theoretical curve is shown in Fig. 2.1. The values of the potential scattering radius and the strength function S_0, which have the values 9.6×10^{-13} cm and $0.97^3 \times 10^{-4}$ $(eV)^{-1/2}$ respectively, correspond well with the values obtained in the unresolved resonance range.

The main level density parameter for determining the energy dependence of the average distance between levels was derived from the values in the resolved resonance range $\langle D_{ev} \rangle$ taking into account the possible missing levels due to their grouping and the insufficiently sensitive equipment [39].

As mentioned earlier, the set of transitional states, is based primarily on the assumptions of Lynn [46]; however, these have been adjusted slightly so that on the average, the group-averaged theoretical cross-sections (i.e. (n,f) + (n,γf)) give a good description of the average interval fission cross-sections obtained in the first stage (Table 2.2). The set of transitional states used in this evaluation is given in Table 2.4.

The set of transitional states is more extensive than necessary for fission widths, as a knowledge of the values of fission thresholds of the compound nuclei, subsequent to the emission of the dipolar γ-quanta, ($J = J_t \pm 1.0$) is needed for calculation of $[\Gamma_\gamma\rangle$ and $\langle \Gamma_{\gamma f} \rangle$.

A comparison of the experimental data with the smooth fission curve is shown in Fig. 2.2.

It should be noted that the systematics of the radiation width dependence, without considering the (n,γf)-process, gives a value of 39 meV for the radiation width of ^{233}U. Using a value of 32 meV for the radiation width to describe α data, and taking the

(n,γf)-process into consideration, gives results which are in good agreement with systematics.

The next stage in the evaluation consisted of a detailed description of the group-averaged cross-sections. Starting from the fact that the average fission widths are significantly greater than the radiation widths, it was assumed that the fluctuations in the average fission cross-sections in the given intervals correspond almost entirely to the power function fluctuations, and should correspond entirely in the broad intervals where there is little variation in the average fission widths. Fitting the group-averaged total cross-sections by varying the strength function S_0 has shown that this leads to an almost total agreement in respect of the fission cross-section. In this connection, in the range up to 2 keV, where the intervals are not wide enough, which causes the average fission width to fluctuate significantly. The average fission widths were also fitted to agree with the experimental values $\langle\sigma_\gamma\rangle/\langle\sigma_f\rangle$ (Table 2.3). It was then assumed that the remaining discrepancy between the group-averaged cross-sections and those calculated by fitting of $\langle\sigma_t\rangle$ was the result of errors in the average interval cross-sections $\langle\sigma_f\rangle$ and $\langle\sigma_t\rangle$ obtained from analysis of the experimental data. Therefore, the quantities $\langle\sigma_f\rangle$ and $\langle\sigma_t\rangle$ were shifted to the same part of the dispersion region before the correspondence of the $\langle\sigma_f\rangle$ values with the calculated fission cross-section which were fitted to $\langle\sigma_t\rangle_{ev}$. The values for $\langle\sigma_f\rangle_{ev}$ and $\langle\sigma_t\rangle_{ev}$ thus obtained were considered to be evaluated.

We note that the two final data points in the Pattenden measurement (Ref. [15]) were not explainable from a physics point of view and were included in the present calculations. Thus, in the 6-40 keV energy range the data for σ_t were missing. Evaluated group-averaged values of the fission cross-sections were thus obtained, and the values of $\langle\sigma_t\rangle_{ev}$ were chosen in such a way that the fitted fission cross-section corresponded with $\langle\sigma_f\rangle$.

The evaluated cross-sections are given in Table 2.5, the average resonance parameters describing these cross-sections are given in Tables 2.6-2.10.

Let us note the following concerning calculation of the (n,γf)-process cross-section. We assume that the width of the (n,γf)-process, as that for the (n,γ), has an infinite number of degrees of freedom which requires that the total gamma ray emission cross-section be calculated and then broken down in proportion to the width of the radiation capture and that of the (n,γf)-process.

The ENDF/B format does not allow calculations to be made in this way; consequently, the cross-sections in the ENDF/B format requires that the (n,γf) width be added to the (n,f) width, and that a determination of the total fission cross-section be made subsequently. Cross-sections obtained in this way differ by less than 0.1% from those that are calculated. The number of degrees of freedom of υ in a χ^2-distributions, to which also include the (n,γ) and (n,γf) widths is infinite. The values of υ for the elastic scattering and fission processes are given in Table 2.11.

2.4. Comparison with other evaluations

Comparison of the average ^{233}U resonance parameters in the present paper with the JENDL-2 evaluation (Ref. [48]) show that the given average distance between levels $\langle D \rangle_{obs}$ = 0.42 eV is significantly less than the value 0.68 eV used in JENDL-2. We consider this value of $\langle D \rangle$ to be more reliable as it is obtained from analysis of experimentally observed distributions of distances between levels of neutron widths using the hypothesis of missing levels due to their low numbers and grouping [47].

The strength functions $S_0 = 0.99 \times 10^{-4}$ eV$^{1/2}$ and $S_1 = 1.54 \times 10^{-4}$ eV$^{1/2}$ given in this paper are ~20% higher than those used in the JENDL-2 evaluation [48].

The average radiation capture width, which is assumed to be equal to 32 meV corresponds to a value of $\langle \Gamma\gamma \rangle$ = 39 meV derived from systematics in the evaluation reported in Ref. [50] if one considers that the average width of the(n,γf) process is equal in these calculations to ~7 meV, and that systematics do not take the reduction in the value of the radiative capture width into consideration at the expense of competing processes.

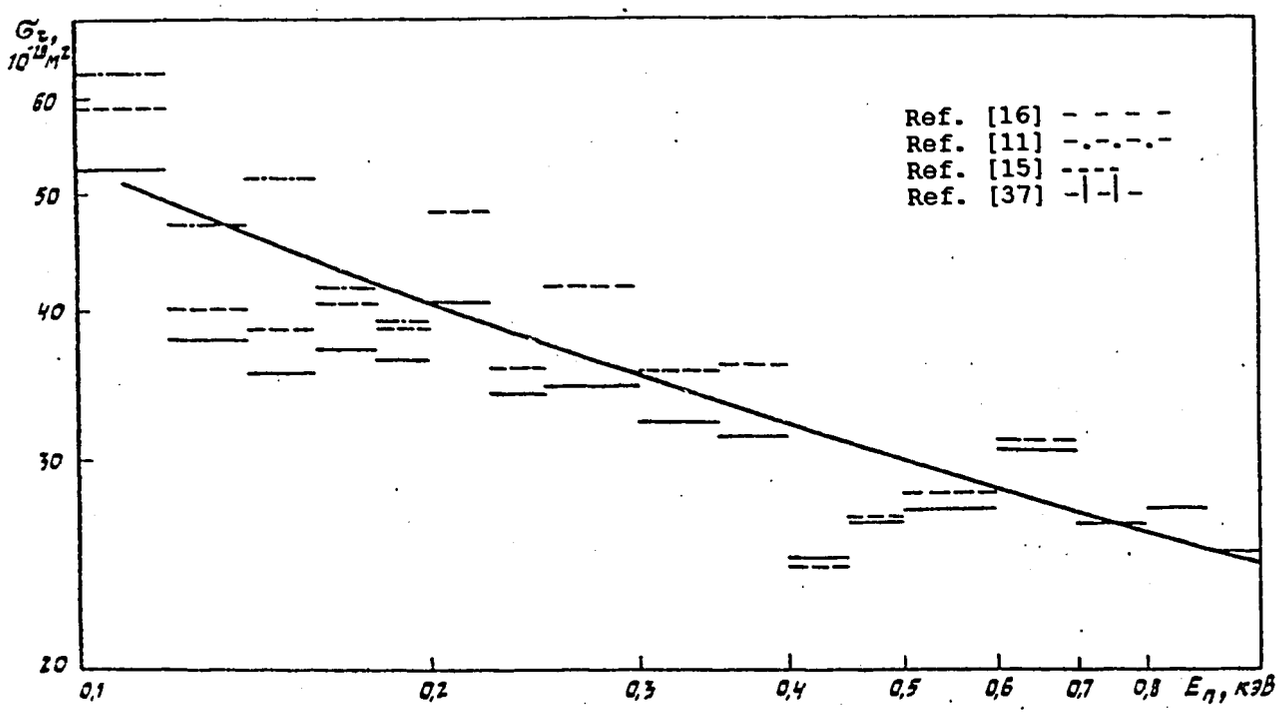

Fig. 2.1 Comparison of smooth calculated values of the total cross-section (continuous line) with interval averaged experimental data

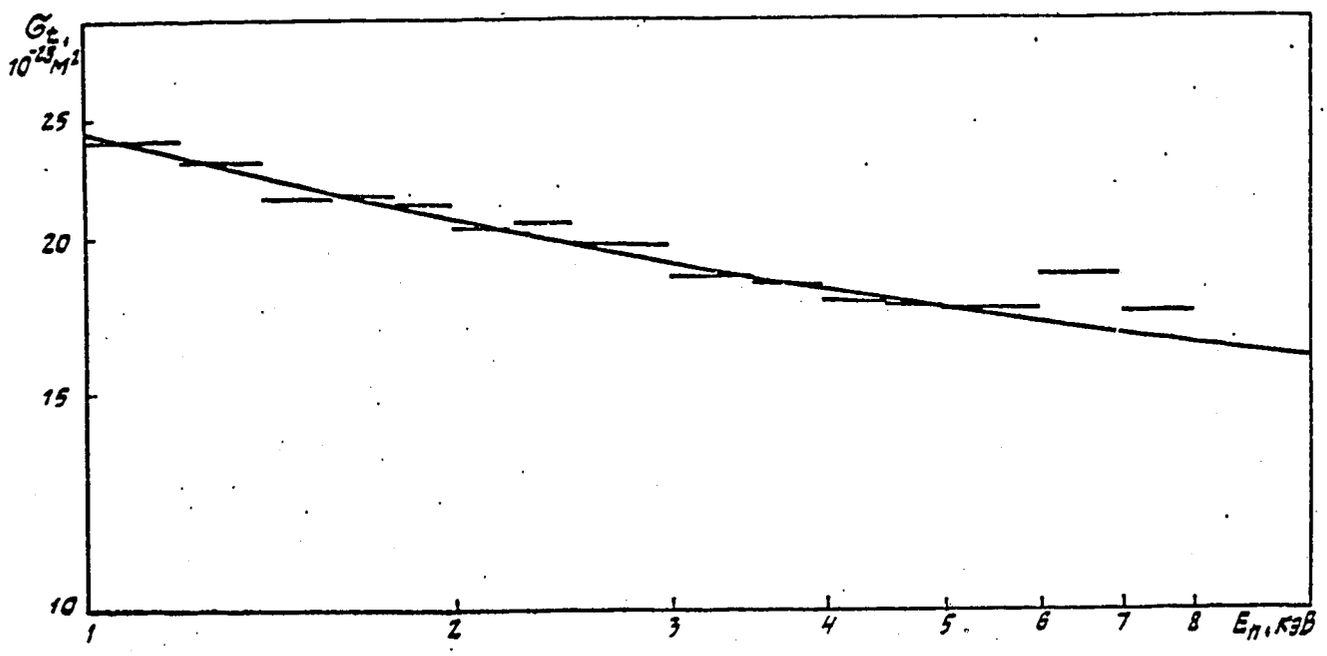

Fig. 2.1 (continued)

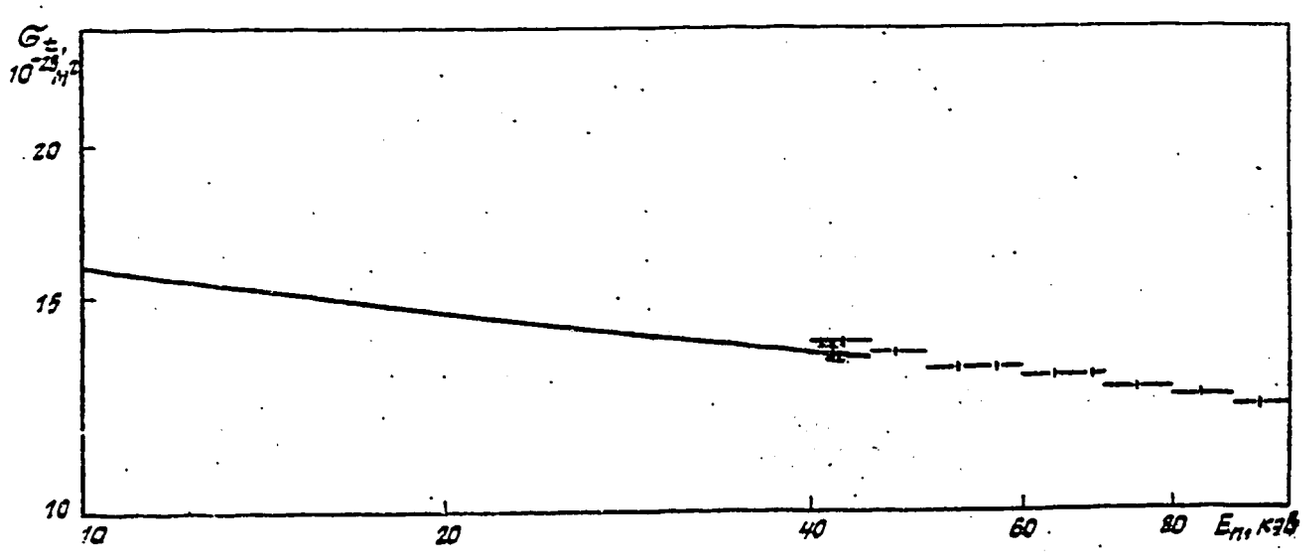

Fig. 2.1 (concluded)

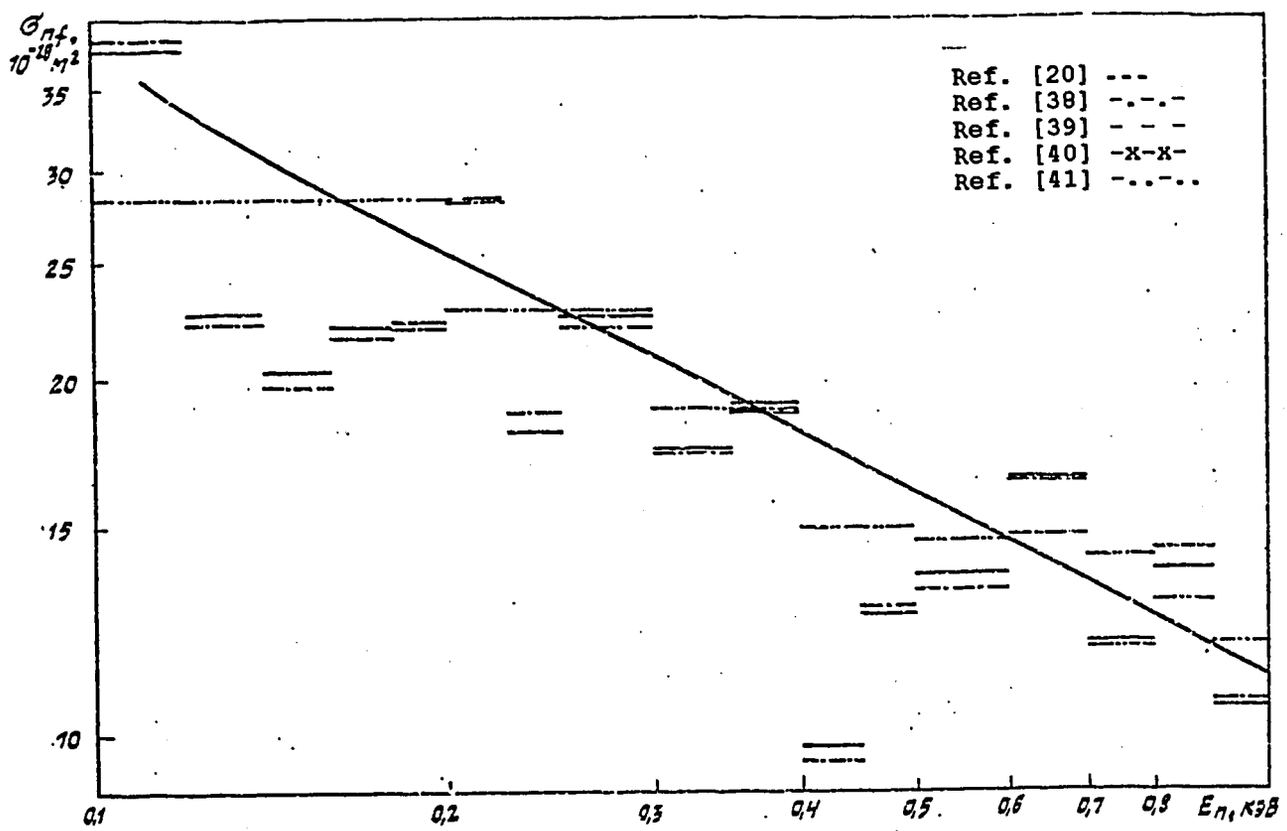

Fig. 2.2 Comparison of the calculated sum of the $\sigma_{n\gamma f}$ and σ_{nf} cross-sections (continuous line) with the interval averaged fission cross-section data

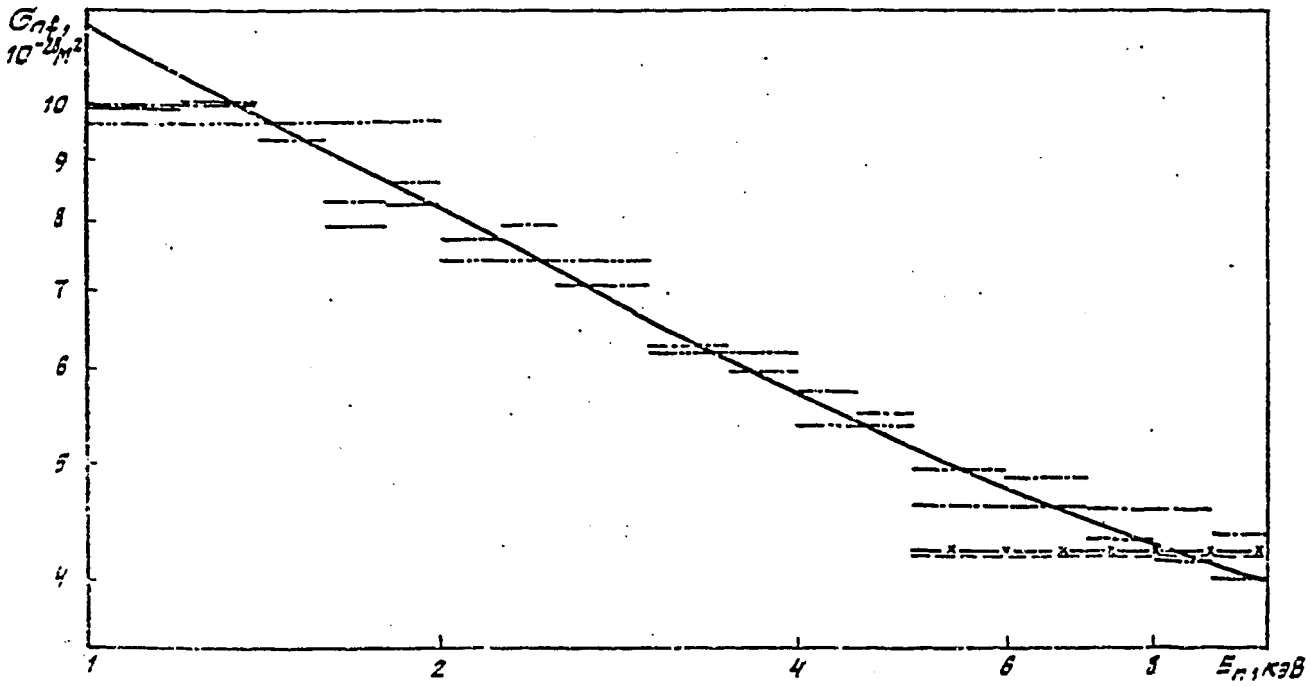

Fig. 2.2 (continued)

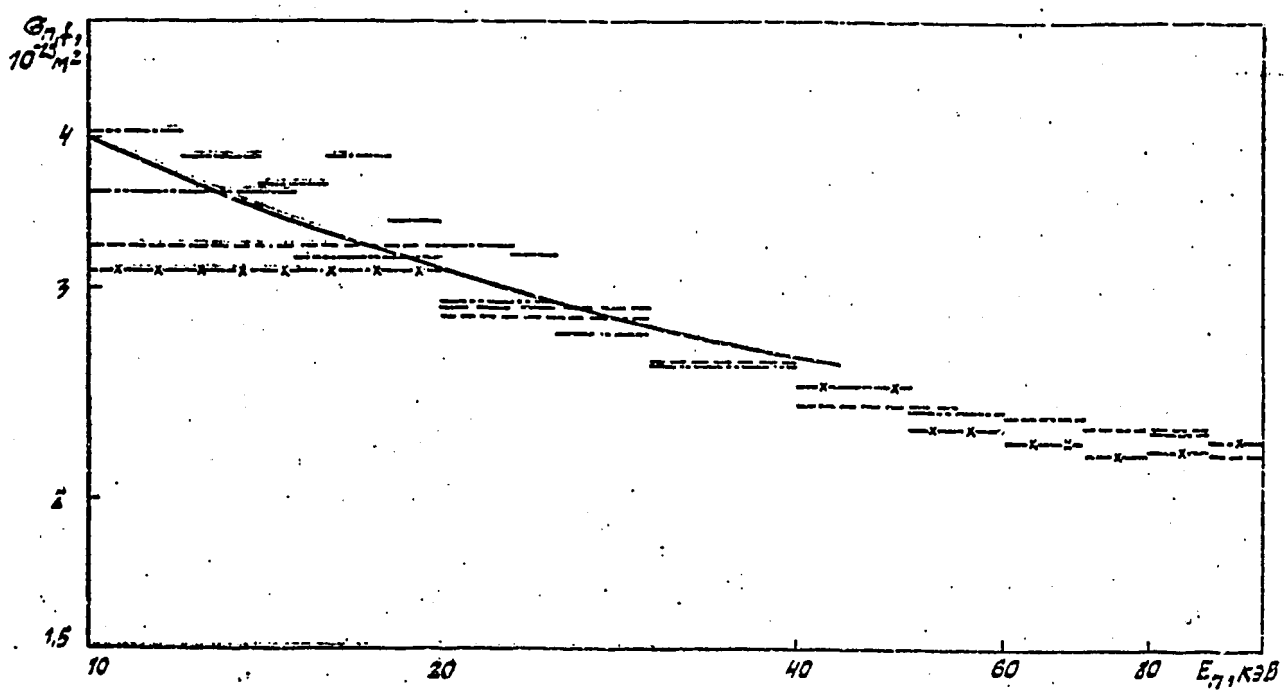

Fig. 2.2 (concluded)

Table 2:1
Interval averaged total cross-section of ^{233}U

$E_{min} - E_{max}$, кэВ	$\langle\sigma_t\rangle$, 10^{-28} м^2	$E_{min} - E_{max}$, кэВ	$\langle\sigma_t\rangle$, 10^{-28} м^2
I	2	3	4
0,I0-0,I2	55,73	I,4-I,6	2I,54
0,I2-0,I4	39,08	I,6-I,8	2I,67
0,I4-0,I6	36,97	I,8-2,0	2I,25
0,I6-0,I8	38,77	2,0-2,25	20,37
0,I8-0,20	37,50	2,25-2,5	20,52
0,20-0,225	44,5I	2,5-3,0	I9,67
0,225-0,25	34,83	3,0-3,5	I8,58
0,25-0,30	38,I5	3,5-4,0	I8,3I
0,30-0,35	33,88	4,0-4,5	I7,69
0,35-0,40	33,62	4,5-5,0	I7,60
0,40-0,45	24,58	5,0-6,0	I7,53
0,45-0,50	26,74	6,0-7,0	I8,67
0,50-0,60	27,62	7,0-8,0	I7,42
0,60-0,70	30,82	40-50	I3,63
0,70-0,80	26,39	50-60	I3,I2
0,80-0,90	27,32	60-70	I2,9I
0,90-I,00	25,I2	70-80	I2,6I
I,0-I,2	23,96	80-90	I2,4I
I,2-I,4	23,06	90-I00	I2,I8

Table 2.2
Interval averaged fission cross-section of ^{233}U

$E_{min} - E_{max}$, кэВ	$\langle\sigma_f\rangle$, 10^{-28} м^2	$E_{min} - E_{max}$, кэВ	$\langle\sigma_f\rangle$, 10^{-28} м^2
I	2	3	4
0,I0-0,I2	40,62	2,0-2,25	7,65
0,I2-0,I4	23,84	2,25-2,5	7,39
0,I4-0,I6	2I,22	2,5-3,0	7,03
0,I6-0,I8	23,2I	3,0-3,5	6,33
0,I8-0,20	23,52	3,5-4,0	6,0I
0,20-0,225	28,22	4,0-4,5	5,65
0,225-0,25	I8,30	4,5-5,0	5,33
0,25-0,30	2I,74	5,0-6,0	4,73
0,30-0,35	I7,70	6,0-7,0	4,54
0,35-0,40	I9,28	7,0-8,0	4,27
0,40-0,45	I0,92	8,0-9,0	4,I3
0,45-0,50	I4,46	9,0-I0,0	3,98
0,50-0,60	I3,98	I0-I2	3,59
0,60-0,70	I5,56	I2-I4	3,44
0,70-0,80	I3,00	I4-I6	3,20
0,80-0,90	I3,29	I6-I8	3,30
0,90-I,0	II,47	I8-20	2,9I
I,0-I,2	I0,36	20-22,5	3,02
I,2-I,4	I0,4I	22,5-25	2,96
I,4-I,6	9,59	25-30	2,79
I,6-I,8	8,45	30-40	2,59
I,8-2,0	8,79	40-50	2,48

Table 2.3
Ratio of the interval averaged cross-sections $\langle\sigma_\gamma\rangle/\langle\sigma_f\rangle$

$E_{min}-E_{max}$, кэВ	$\langle\sigma_\gamma\rangle/\langle\sigma_f\rangle$	$E_{min}-E_{max}$, кэВ	$\langle\sigma_\gamma\rangle/\langle\sigma_f\rangle$
0,I0-0,I2	0,I44	0,45-0,50	0,II6
0,I2-0,I4	0,I23	0,50-0,60	0,I62
0,I4-0,I6	0,I87	0,60-0,70	0,II5
0,I6-0,I8	0,I3I	0,70-0,80	0,I26
0,I8-0,20	0,082	0,80-0,90	0,II4
0,20-0,225	0,I66	0,90-I,00	0,I26
0,225-0,25	0,III	I,0-I,2	0,077
0,25-0,30	0,I26	I,2-I,4	0,092
0,30-0,35	0,092	I,4-I,6	0,087
0,35-0,40	0,069	I,6-I,8	0,I38
0,40-0,45	0,053	I,8-2,0	0,I22

Table 2.4
Scheme of transitional fission states

E_f*, MeV	Spin and parity oof transitional states				
-1.50	0+	2+	4+		
-1.00	1-	3-			
-0.80	2+	3+	4+	5+	
-0.60	1-	2-	3-	4-	
-0.30	2+	3+	2-	3-	4-
-0.05	1+	2+	3+		
0.0	1-	2-	3-	4-	

The values were derived from neutron binding energies

Table 2.5
Evaluated ^{233}U neutron cross-sections in the unresolved resonance region, 10^{-28} m^2

$E_{min}-E_{max}$, кэВ	$\langle\sigma_t\rangle$	$\langle\sigma_n\rangle$	$\langle\sigma_f\rangle$	$\langle\sigma_{\gamma f}\rangle$	$\langle\sigma_\gamma\rangle$
I	2	3	4	5	6
0,I0-0,I2	57,080	II,987	38,3I7	I,I07	5,669
0,I2-0,I4	38,790	II,7I8	23,509	0,593	2,970
0,I4-0,I6	37,020	II,786	20,402	0,770	4,062
0,I6-0,I8	38,390	II,762	22,943	0,6I0	3,075
0,I8-0,20	37,330	II,697	23,247	0,42I	I,965
0,20-0,225	44,760	I2,036	27,096	0,907	4,72I
0,225-0,25	33,430	II,7[illegible]5	I9,095	0,443	2,I77
0,25-0,30	37,240	II,837	2I,983	0,569	2,85I
0,30-0,35	32,430	II,7I0	I8,623	0,366	I,73I
0,35-0,40	32,950	II,696	I9,558	0,3I0	I,386
0,40-0,45	23,8I0	II,585	II,459	0,I50	0,6I6
0,45-0,50	27,280	II,700	I3,640	0,329	I,6II
0,50-0,60	27,850	II,807	I3,34I	0,440	2,262
0,60-0,70	29,990	II,825	I5,894	0,385	I,886
0,70-0,80	26,390	II,757	I2,67I	0,330	I,632
0,80-0,90	26,950	II,778	I3,287	0,32I	I,564
0,90-I,00	24,900	II,748	II,370	0,30I	I,48I
I,0-I,2	23,360	II,629	I0,700	0,I89	0,842
I,2-I,4	23,040	II,657	I0,22I	0,208	0,954
I,4-I,6	2I,790	II,623	9,I68	0,I8I	0,8I8
I,6-I,8	2I,460	II,693	8,420	0,23I	I,II6
I,8-2,0	2I,400	II,688	8,440	0,220	I,052
2,0-2,25	20,270	II,639	7,536	0,I92	0,903
2,25-2,5	20,490	II,654	7,7I6	0,I97	0,923
2,5-3,0	I9,570	II,6I9	6,940	0,I79	0,832
3,0-3,5	I8,620	II,578	6,I42	0,I62	0,738
3,5-4,0	I8,300	II,562	5,876	0,I56	0,706
4,0-4,5	I7,7I0	II,530	5,385	0,I46	0,649
4,5-5,0	I7,540	II,5I5	5,249	0,I43	0,633
5,0-6,0	I7,I40	II,483	4,925	0,I37	0,595
6,0-7,0	I6,5I0	II,436	4,4I2	0,I27	0,535
7,0-8,0	I6,I70	II,398	4,I45	0,I22	0,505
8,0-9,0	I5,980	II,365	4,006	0,I20	0,489
9,0-I0	I5,780	II,332	3,858	0,II8	0,472
I0-I2	I5,300	II,279	3,48I	0,III	0,429
I2-I4	I5,070	II,220	3,328	0,II0	0,4I2
I4-I6	I4,750	II,I62	3,095	0,I07	0,386
I6-I8	I4,8I0	II,I08	3,I94	0,III	0,397
I8-20	I4,330	II,060	2,8II	0,I04	0,355
20-22,5	I4,370	I0,997	2,92I	0,I02	0,350
22,5-25	I4,240	I0,935	2,860	0,I02	0,343
25-30	I3,940	I0,843	2,698	0,095	0,304
30-40	I3,570	I0,698	2,493	0,095	0,284
40-50	I3,280	I0,524	2,385	0,097	0,274

Table 2.6
Evaluated average distances between levels of the compound ^{234}U nucleus, eV

$E_{min}-E_{max}$, кэВ	$\langle D_1 \rangle$	$\langle D_2 \rangle$	$\langle D_3 \rangle$	$\langle D_4 \rangle$
I	2	3	4	5
0,I0-0,I2	I,592	0,983	0,733	0,604
0,I2-0,I4	I,592	0,983	0,733	0,604
0,I4-0,I6	I,592	0,983	0,733	0,604
0,I6-0,I8	I,592	0,983	0,733	0,604
0,I8-0,20	I,592	0,983	0,733	0,604
0,20-0,225	I,592	0,983	0,733	0,604
0,225-0,25	I,592	0,983	0,733	0,604
0,25-0,30	I,592	0,983	0,733	0,603
0,30-0,35	I,592	0,983	0,733	0,603
0,35-0,40	I,59I	0,983	0,733	0,603
0,40-0,45	I,59I	0,982	0,733	0,603
0,45-0,50	I,59I	0,982	0,732	0,603
0,50-0,60	I,59I	0,982	0,732	0,603
0,60-0,70	I,59I	0,982	0,732	0,603
0,70-0,80	I,590	0,982	0,732	0,603
0,80-0,90	I,590	0,982	0,732	0,603
0,90-I,00	I,590	0,98I	0,732	0,603
I,0-I,2	I,589	0,98I	0,732	0,602
I,2-I,4	I,589	0,98I	0,73I	0,602
I,4-I,6	I,588	0,980	0,73I	0,602
I,6-I,8	I,587	0,980	0,73I	0,602
I,8-2,0	I,587	0,980	0,730	0,602
2,0-2,25	I,586	0,979	0,730	0,60I
2,25-2,5	I,585	0,979	0,730	0,60I
2,5-3,0	I,584	0,978	0,729	0,60I
3,0-3,5	I,583	0,977	0,729	0,600
3,5-4,0	I,58I	0,976	0,728	0,599
4,0-4,5	I,580	0,975	0,727	0,599
4,5-5,0	I,578	0,974	0,726	0,598
5,0-6,0	I,576	0,973	0,725	0,597
6,0-7,0	I,573	0,97I	0,724	0,596
7,0-8,0	I,570	0,969	0,723	0,595
8,0-9,0	I,567	0,967	0,72I	0,594
9,0-I0	I,564	0,965	0,720	0,593
I0-I2	I,559	0,963	0,7I8	0,59I
I2-I4	I,553	0,959	0,7I5	0,589
I4-I6	I,547	0,955	0,7I2	0,586
I6-I8	I,54I	0,952	0,709	0,584
I8-20	I,535	0,948	0,707	0,582
20-22,5	I,529	0,944	0,704	0,579
22,5-25	I,52I	0,939	0,700	0,577
25-30	I,5I0	0,932	0,695	0,572
30-40	I,489	0,9I9	0,685	0,564
40-50	I,460	0,902	0,672	0,553

Table 2.7

Evaluated average ^{233}U neutron widths, meV

$E_{min}-E_{max}$, кэВ	$\langle \Gamma^1_{n_1-} \rangle$	$\langle \Gamma^1_{n_2} \rangle$	$\langle \Gamma^0_{n_2+} \rangle$	$\langle \Gamma^0_{n_3+} \rangle$	$\langle \Gamma^1_{n_3-} \rangle$	$\langle \Gamma^1_{n_4-} \rangle$
I	2	3	4	5	6	7
0,I0–0,I2	0,00I	0,00I	I,I92	0,889	0,00I	0,000
0,I2–0,I4	0,00I	0,002	0,842	0,627	0,00I	0,000
0,I4–0,I6	0,002	0,002	0,908	0,677	0,00I	0,00I
0,I6–0,I8	0,002	0,002	I,084	0,808	0,002	0,00I
0,I8–0,20	0,002	0,003	I,I64	0,868	0,002	0,00I
0,20–0,225	0,003	0,003	I,678	I,25I	0,002	0,00I
0,225–0,25	0,003	0,004	I,233	0,920	0,003	0,00I
0,25–0,30	0,004	0,005	I,678	I,25I	0,003	0,00I
0,30–0,35	0,005	0,006	I,6I0	I,200	0,004	0,002
0,35–0,40	0,006	0,007	I,904	I,420	0,005	0,002
0,40–0,45	0,007	0,009	I,230	0,9I7	0,007	0,003
0,45–0,50	0,008	0,0I0	I,768	I,3I8	0,008	0,003
0,50–0,60	0,0II	0,0I3	2,I22	I,582	0,0I0	0,004
0,60–0,70	0,0I4	0,0I7	2,84I	2,II8	0,0I2	0,005
0,70–0,80	0,0I7	0,02I	2,632	I,962	0,0I5	0,006
0,80–0,90	0,020	0,025	3,097	2,309	0,0I9	0,008
0,90–I,00	0,024	0,030	2,994	2,233	0,022	0,009
I,0–I,2	0,030	0,037	3,06I	2,282	0,027	0,0II
I,2–I,4	0,038	0,047	3,5I7	2,623	0,035	0,0I5
I,4–I,6	0,047	0,058	3,608	2,690	0,044	0,0I8
I,6–I,8	0,057	0,070	3,954	2,948	0,053	0,022
I,8–2,0	0,067	0,083	4,393	3,275	0,062	0,026
2,0–2,25	0,080	0,098	4,334	3,23I	0,073	0,030
2,25–2,5	0,094	0,II6	4,972	3,707	0,086	0,036
2,5–3,0	0,II7	0,I44	5,I46	3,837	0,I08	0,044
3,0–3,5	0,I50	0,I85	5,335	3,977	0,I38	0,057
3,5–4,0	0,I85	0,228	5,867	4,375	0,I70	0,070
4,0–4,5	0,223	0,275	6,04I	4,504	0,205	0,084
4,5–5,0	0,262	0,324	6,560	4,89I	0,242	0,099
5,0–6,0	0,326	0,402	7,064	5,267	0,300	0,I23
6,0–7,0	0,4I6	0,5I4	7,350	5,480	0,383	0,I58
7,0–8,0	0,5I3	0,634	7,865	5,864	0,472	0,I95
8,0–9,0	0,6I6	0,76I	8,533	6,362	0,567	0,234
9,0–I0	0,724	0,894	9,086	6,774	0,667	0,274
I0–I2	0,895	I,I05	9,222	6,875	0,824	0,339
I2–I4	I,I38	I,406	I0,209	7,6II	I,048	0,43I
I4–I6	I,397	I,724	I0,6I7	7,9I5	I,286	0,529
I6–I8	I,668	2,059	I2,434	9,270	I,535	0,632
I8–20	I,95I	2,409	II,558	8,6I7	I,796	0,739
20–22,5	2,28I	2,8I6	I3,344	9,948	2,I00	[illegible]
22,5–25	2,66I	3,286	I4,289	I0,653	2,450	[illegible]
25–30	3,254	4,0I8	I4,587	I0,875	[illegible]	[illegible]
30–40	4,502	5,559	I5,733	II,729	4,I44	I,706
40–50	6,25I	7,7I8	I7,942	I3,375	5,753	2,368

Table 2.8
Evaluated average ^{233}U fission widths, meV

$E_{min}-E_{max}$, кэВ	$\langle\Gamma_{f_{1-}}\rangle$	$\langle\Gamma_{f_{2-}}\rangle$	$\langle\Gamma_{f_{2+}}\rangle$	$\langle\Gamma_{f_{3+}}\rangle$	$\langle\Gamma_{f_{3-}}\rangle$	$\langle\Gamma_{f_{4-}}\rangle$
I	2	3	4	5	6	7
0,I0-0,I2	632,423	380,576	554,899	283,48I	400,397	233,687
0,I2-0,I4	632,4I0	380,570	554,865	366,248	400,388	233,683
0,I4-0,I6	632,406	380,569	554,880	I77,683	400,385	233,683
0,I6-0,I8	632,382	380,55I	554,849	332,445	400,369	233,675
0,I8-0,20	632,369	380,545	554,836	728,462	400,360	233,67I
0,20-0,225	632,357	380,540	554,823	2I7,780	400,352	233,668
0,225-0,25	632,348	380,537	554,8I3	432,834	400,345	233,666
0,25-0,30	632,329	380,529	554,793	349,224	400,325	233,66I
0,30-0,35	632,280	380,504	554,746	6I3,4I4	400,292	233,643
0,35-0,40	632,252	380,492	554,7I7	I027,573	400,273	233,635
0,40-0,45	632,223	380,479	554,687	2055,I79	400,252	233,627
0,45-0,50	632,I95	380,466	554,657	407,764	400,233	233,620
0,50-0,60	632,I47	380,444	554,608	226,4I2	400,I99	233,606
0,60-0,70	632,080	380,4I3	554,540	40I,970	400,I53	233,587
0,70-0,80	632,0I2	380,382	554,472	35I,974	400,I07	233,568
0,80-0,90	63I,955	380,356	554,4I3	407,354	400,067	233,552
0,90-I,00	63I,888	380,325	554,345	344,982	400,020	233,533
I,0-I,2	63I,792	380,28I	554,247	846,342	399,953	233,505
I,2-I,4	63I,657	380,2I9	554,III	6I3,022	399,86I	233,467
I,4-I,6	63I,533	380,I6I	553,983	668,872	399,774	233,429
I,6-I,8	63I,407	380,I04	553,856	334,296	399,687	233,394
I,8-2,0	63I,274	380,042	553,720	370,28I	399,595	233,355
2,0-2,25	63I,I30	379,976	553,573	396,450	399,489	233,3I5
2,25-2,5	630,977	379,906	553,4I6	396,37I	399,383	233,272
2,5-3,0	630,737	379,795	553,I70	396,247	399,2I6	233,200
3,0-3,5	630,4I0	379,643	552,837	396,077	398,990	233,I07
3,5-4,0	630,094	379,492	552,505	395,9I3	398,770	233,0I4
4,0-4,5	629,777	379,345	552,I8I	395,742	398,544	232,924
4,5-5,0	629,460	379,I98	55I,856	395,577	398,324	232,830
5,0-6,0	628,97I	378,970	55I,356	395,320	397,984	232,690
6,0-7,0	628,328	378,669	550,697	394,974	397,53I	232,502
7,0-8,0	627,695	378,368	550,037	394,632	397,084	232,3I7
8,0-9,0	627,05I	378,065	549,376	394,289	396,637	232,I27
9,0-I0	626,407	377,76I	548,7I4	393,938	396,I83	23I,937
I0-I2	625,447	377,307	547,725	393,4I9	395,5I4	23I,665
I2-I4	624,I58	376,693	546,395	392,7I0	394,6I0	23I,27I
I4-I6	622,878	376,075	545,062	392,000	393,7I0	230,89I
I6-I8	62I,598	375,459	543,735	39I,283	392,809	230,506
I8-20	620,305	374,827	542,388	390,552	39I,90I	230,II4
20-22,5	6I8,858	374,I2I	540,883	389,732	390,888	229,678
22,5-25	6I7,253	373,335	539,2II	388,802	389,753	229,I85
25-30	6I4,83I	372,I32	536,678	387,385	388,046	228,439
30-40	609,985	369,696	53I,60I	384,498	384,63I	226,926
40-50	603,479	366,353	524,763	380,503	380,042	224,850

Table 2.9
Evaluated average ^{233}U (n,γf) widths meV

$E_{min}-E_{max}$, кэВ	$\langle\Gamma_{\gamma f_{1-}}\rangle$	$\langle\Gamma_{\gamma f_{2-}}\rangle$	$\langle\Gamma_{\gamma f_{2+}}\rangle$	$\langle\Gamma_{\gamma f_{3+}}\rangle$	$\langle\Gamma_{\gamma f_{3-}}\rangle$	$\langle\Gamma_{\gamma f_{4-}}\rangle$
I	2	3	4	5	6	7
0,I0-0,I2	I5,I34	I0,359	8,442	5,52I	I6,II2	I0,827
0,I2-0,I4	I5,I35	I0,359	8,443	5,52I	I6,II3	I0,827
0,I4-0,I6	I5,I35	I0,360	8,443	5,522	I6,II3	I0,828
0,I6-0,I8	I5,I35	I0,360	8,443	5,522	I6,II3	I0,828
0,I8-0,20	I5,I36	I0,360	8,443	5,522	I6,II4	I0,829
0,20-0,225	I5,I36	I0,360	8,444	5,522	I6,II4	I0,829
0,225-0,25	I5,I36	I0,36I	8,444	5,523	I6,II5	I0,830
0,25-0,30	I5,I37	I0,362	8,445	5,523	I6,II6	I0,830
0,30-0,35	I5,I38	I0,362	8,445	5,524	I6,II7	I0,83I
0,35-0,40	I5,I39	I0,363	8,446	5,524	I6,II8	I0,832
0,40-0,45	I5,I39	I0,364	8,447	5,525	I6,II9	I0,833
0,45-0,50	I5,I40	I0,365	8,448	5,525	I6,I20	I0,834
0,50-0,60	I5,I4I	I0,366	8,449	5,526	I6,I2I	I0,835
0,60-0,70	I5,I43	I0,367	8,450	5,527	I6,I24	I0,837
0,70-0,80	I5,I44	I0,369	8,452	5,529	I6,I26	I0,839
0,80-0,90	I5,I46	I0,370	8,453	5,530	I6,I28	I0,840
0,90-I,00	I5,I48	I0,372	8,455	5,53I	I6,I30	I0,842
I,0-I,2	I5,I50	I0,374	8,457	5,533	I6,I33	I0,845
I,2-I,4	I5,I53	I0,377	8,460	5,535	I6,I37	I0,849
I,4-I,6	I5,I56	I0,38I	8,463	5,537	I6,I4I	I0,852
I,6-I,8	I5,I60	I0,384	8,466	5,540	I6,I46	I0,856
I,8-2,0	I5,I63	I0,387	8,469	5,542	I6,I50	I0,859
2,0-2,25	I5,I66	I0,390	8,472	5,545	I6,I54	I0,863
2,25-2,5	I5,I70	I0,394	8,476	5,548	I6,I59	I0,868
2,5-3,0	I5,I76	I0,400	8,482	5,552	I6,I67	I0,875
3,0-3,5	I5,I84	I0,408	8,489	5,558	I6,I78	I0,884
3,5-4,0	I5,I92	I0,4I6	8,497	5,564	I6,I88	I0,893
4,0-4,5	I5,200	I0,424	8,504	5,570	I6,I99	I0,902
4,5-5,0	I5,208	I0,43I	8,5I2	5,576	I6,209	I0,9II
5,0-6,0	I5,220	I0,443	8,523	5,585	I6,225	I0,924
6,0-7,0	I5,235	I0,459	8,538	5,597	I6,245	I0,942
7,0-8,0	I5,25I	I0,474	8,553	5,609	I6,266	I0,960
8,0-9,0	I5,267	I0,490	8,568	5,62I	I6,287	I0,979
9,0-I0	I5,283	I0,506	8,583	5,632	I6,308	I0,997
I0-I2	I5,306	I0,529	8,606	5,650	I6,339	II,024
I2-I4	I5,338	I0,55I	8,636	5,674	I6,38I	II,060
I4-I6	I5,370	I0,60I	8,7I9	5,738	I6,430	II,I02
I6-I8	I5,402	I0,632	8,750	5,762	I6,472	II,I39
I8-20	I5,433	I0,664	8,78I	5,787	I6,5I4	II,I35
20-22,5	I5,469	I0,700	8,8I6	5,8I5	I6,56I	II,2I7
22,5-25	I5,508	I0,739	8,855	5,846	I6,6I4	II,262
25-30	I5,568	I0,799	8,9I4	5,892	I6,693	II,332
30-40	I5,687	I0,9I9	9,03I	5,986	I6,85I	II,47I
40-50	I5,846	II,079	9,I66	6,II3	I7,063	II,657

Table 2.10

Evaluated average ^{233}U radiation capture widths meV

$E_{min}-E_{max}$, кэВ	$\langle\Gamma_{\gamma_{1-}}\rangle$	$\langle\Gamma_{\gamma_{2-}}\rangle$	$\langle\Gamma_{\gamma_{2+}}\rangle$	$\langle\Gamma_{\gamma_{3+}}\rangle$	$\langle\Gamma_{\gamma_{3-}}\rangle$	$\langle\Gamma_{\gamma_{4-}}\rangle$
I	2	3	4	5	6	7
0,I0-0,I2	24,452	28,796	30,7I2	33,006	22,4I5	26,896
0,I2-0,I4	24,452	28,796	30,7I2	33,006	22,4I5	26,896
0,I4-0,I6	24,452	28,796	30,7I3	33,007	22,4I5	26,897
0,I6-0,I8	24,452	28,795	30,7I2	33,006	22,4I5	26,896
0,I8-0,20	24,452	28,795	30,7I2	33,006	22,4I4	26,896
0,20-0,225	24,452	28,795	30,7I2	33,006	22,4I4	26,896
0,225-0,25	24,452	28,795	30,7I2	33,007	22,4I4	26,896
0,25-0,30	24,452	28,795	30,7I2	33,007	22,4I4	26,896
0,30-0,35	24,45I	28,795	30,7I2	33,006	22,4I3	26,895
0,35-0,40	24,452	28,795	30,7I2	33,007	22,4I3	26,895
0,40-0,45	24,45I	28,795	30,7I2	33,007	22,4I3	26,895
0,45-0,50	24,452	28,795	30,7I2	33,007	22,4I3	26,895
0,50-0,60	24,452	28,795	30,7I2	33,007	22,4I2	26,895
0,60-0,70	24,45I	28,795	30,7I2	33,008	22,4II	26,894
0,70-0,80	24,45I	28,794	30,7I2	33,008	22,4II	26,894
0,80-0,90	24,45I	28,795	30,7I2	33,008	22,4I0	26,894
0,90-I,00	24,45I	28,794	30,7I2	33,008	22,4I0	26,893
I,0-I,2	24,45I	28,794	30,7I2	33,009	22,409	26,893
I,2-I,4	24,450	28,794	30,7II	33,009	22,407	26,892
I,4-I,6	24,450	28,794	30,7II	33,0I0	22,406	26,89I
I,6-I,8	24,450	28,794	30,7I2	33,0II	22,405	26,89I
I,8-2,0	24,450	28,793	30,7II	33,0II	22,403	26,890
2,0-2,25	24,449	28,793	30,7II	33,0II	22,402	26,889
2,25-2,5	24,449	28,793	30,7II	33,0I2	22,400	26,888
2,5-3,0	24,449	28,793	30,7II	33,0I3	22,398	26,887
3,0-3,5	24,448	28,792	30,7I0	33,0I4	22,395	26,885
3,5-4,0	24,447	28,79I	30,7I0	33,0I6	22,392	26,883
4,0-4,5	24,447	28,79I	30,7I0	33,0I7	22,388	26,882
4,5-5,0	24,446	28,790	30,7I0	33,0I9	22,385	26,880
5,0-6,0	24,445	28,789	30,709	33,020	22,38I	26,877
6,0-7,0	24,443	28,788	30,708	33,022	22,374	26,873
7,0-8,0	24,442	28,787	30,708	33,025	22,367	26,870
8,0-9,0	24,44I	28,786	30,707	33,028	22,36I	26,866
9,0-I0	24,439	28,784	30,707	33,030	22,354	26,862
I0-I2	24,438	28,783	30,706	33,034	22,345	26,856
I2-I4	24,435	28,780	30,704	33,039	22,332	26,849
I4-I6	24,432	28,769	30,650	33,005	22,3I3	26,836
I6-I8	24,430	28,767	30,649	33,009	22,300	26,829
I8-20	24,427	28,764	30,646	33,0I3	22,287	26,82I
20-22,5	24,424	28,76I	30,644	33,0I9	22,272	26,8I2
22,5-25	24,42I	28,758	30,642	33,024	22,256	26,803
25-30	24,4I6	28,753	30,638	33,032	22,23I	26,788
30-40	24,408	28,744	30,63I	33,048	22,I83	26,759
40-50	24,396	28,73I	30,644	33,069	22,II8	26,7I9

Table 2.11
Number of degrees of freedom for χ^2 distribution of average partial widths

ℓ	J^π	υ_n	υ_f			
			Energy ranges, keV			
			0.1-2	2-20	20-25	25-50
1	1-	1	2	3	3	3
1	2-	2	2	2	3	3
0	2+	1	4	4	4	4
0	3+	1	3	3	3	4
1	3-	2	3	3	3	4
1	4-	1	2	2	3	3

3. THE ^{233}U NEUTRON FISSION CROSS-SECTION

The ^{233}U neutron fission cross-section has been studied in some detail in the 0.04-20 MeV neutron energy region (Fig. 3.1). The studies have consisted mainly of measurements relating to the ^{235}U fission cross-section, with only one series of data [49] covering the whole neutron energy range of interest to us. In addition, we do have a little data from absolute measurements at points E_n = 14-15 MeV [50, 51] and E_n = 1.9 MeV [52] and in the 0.13-8 MeV region [53], obtained using various techniques for recording the fission fragments, measuring the neutron flux and converting the fission cross-section ratios into absolute values. The discrepancies between the experimental values would seem to have been due to the fact that systematic errors associated with the various techniques were not taken into account. Even from the data we have, however, it is possible to select a representative set of experiments which agree among themselves within the error limits and can provide a database for evaluation.

3.1. Brief description of the experiments

Using the time-of-flight method, Carlson et al. [49] have measured the ratio of the ^{233}U and ^{235}U fission cross-sections over the widest range of neutron energies - 1 keV-30 MeV. Instead of

an electrostatic accelerator, a linear electron accelerator was used for producing the neutrons. An ionization chamber was used for recording the fission fragments. Two methods were used for normalizing the data: the thermal calibration method and the isotopic impurity method. With the latter method, the ratio of the cross-sections for ^{233}U and ^{235}U was obtained from the ratios of the cross-sections for ^{238}U and ^{233}U and for ^{238}U and ^{235}U. In the 1.75-4 MeV normalization range, with these two methods the normalization coefficients for the energy dependence of the ^{233}U and ^{235}U fission cross-section ratio are different: thermal calibration gives ratios -3.6% higher than those given by the isotopic impurity method. The final normalization coefficient was determined by averaging. The authors' total error level for the ratio varied from ~ 2% at 1 keV to ~ 1.2% in the ~ 1 MeV region, rising to ~ 2.6% at ~ 20 MeV.

Dushin et al. [50] have measured the cross-section for ^{233}U fission by 14.5 MeV neutrons using the time-correlated associated particle method. The reaction $^{3}H(d,n)^{4}He$ was used to produce the neutrons, and a plastic scintillator was used to record the helions associated with the neutrons. An ionization chamber was used to detect the fission fragments. Layer calibration was done by measuring the alpha activity. The error level for the cross-section was 1.7%.

Zasadny et al. [51] have measured the absolute value of the cross-section for ^{233}U fission by 14.62 MeV neutrons. A track detector was used to record the fission fragments. The neutron flux was determined relative to the $^{56}Fe(n,p)^{56}Mn$ activation cross-section. A 4π proportional counter was used to measure the activity. Time-related variations in the neutron flux were taken into account through the use of a boron counter. Microbalances were used to determine the number of nuclei in the layer. The error level for the cross-section was 3.3%.

Kalinin et al. [52] have measured the cross-section for ^{233}U fission by 1.9 MeV neutrons using the time-correlated associated particle method. The reaction $D(\alpha,n)^{3}He$ was used to produce the neutrons. A silicon surface-barrier detector was used to record the helions. The uniformity of the layer was determined from the alpha activity. The error level for the cross-section was 3.8%.

Poenitz [53] has measured the fission cross-section in the 0.13-8.0 MeV energy range. This is the only work in which the absolute fission cross-section values have been measured over such a wide energy range. An ionization chamber was used to record the fission fragments. A total absorption detector was used to measure the neutron flux. The number of nuclei in the layer was determined by measuring the alpha activity. The error level for the cross-section did not exceed 1.8%.

Iyer et al. [54] have measured the ratio of the ^{233}U and ^{238}U fission cross-sections at E_n = 14.1 MeV. Plastic track detectors were used to record the fission fragments. No information is given about the calibration of the fissile layers. The error level for the ratio was 18%.

Meadows has measured the fission cross-section ratio in the 0.1-7.5 MeV neutron energy range [55]. The ionization technique was used to study the energy dependence of the ratio. Absolute ratio values were obtained at four energy points: 1.5, 2.0, 2.5 and 3.0 MeV. The thermal calibration method was used for conversion to absolute values. Calibration by comparing the alpha activity levels of the ^{233}U and ^{235}U layers yields results which agree within the limits of statistical error. The error level for the ratio did not exceed 1%.

Meadows has also measured the fission cross-section ratio at E_n = 14.74 MeV [56] using the method described in Ref. [55]; the reaction $T(D,n)^4He$ was used to produced the neutrons. The error level for the ratio was 0.7%.

Fursov et al. [57] have measured the ^{233}U and ^{235}U fission cross-section ratio in the 0.024-7.4 MeV neutron energy range. The ionization technique was used to study the energy dependence of the ratio. The values thus obtained were normalized to the data produced by measuring the ratio using the glass detector technique in the 0.127-7 MeV energy region. The thermal calibration method was used to convert the data to absolute values. The error level for the cross-section ratio values did not exceed 2.2%.

Kanda et al. [58] have measured the ^{233}U and ^{235}U fission cross-section ratio in the 0.5-7 MeV neutron energy range. The number of nuclei in the ^{233}U layer was determined from the alpha activity level; the number of nuclei in the ^{235}U layer was determined using the thermal calibration method. The error level for the cross-section ratio was 0.7-1.9%.

Shpak et al. [59] have measured the ^{233}U and ^{235}U fission cross-section ratio in the 0.06-3.28 MeV energy region. The fission fragments were recorded using glass detectors in 4π geometry. The thermal calibration method was used to convert the data to absolute values. As the neutron energy rose, the error levels for the ratios decreased from ~1.8% to 1.2% (at E_n = 3.28 MeV).

White et al. have measured the ^{233}U and ^{235}U fission cross-section ratio at the following energy points: 0.04, 0.067, 0.127, 0.312, 0.415 and 0.505 MeV [60]; 1.0, 2.25, 5.4 and 14.1 MeV [61]. An ionization chamber was used to record the fission fragments. The ratio of the numbers of nuclei was determined by comparing the alpha activity levels in the layers. In the renormalization of the data, account must be taken of the new half-life value $T^{*}_{1/2}$. This increases the ratio by 3.6%. The error level for the ratios was ~2%.

Nesterov and Smirenkin [62] have measured the ^{233}U and ^{235}U fission cross-section ratio in the 0.3-2.5 MeV energy range. The measurement technique was similar to the one used later for a wider neutron energy range [57]. The accuracy of the cross section ratio measurements was at the worst 3%.

Pfletchinger and Kappeler [63] have measured the ^{233}U and ^{235}U fission cross-section ratio with an accuracy of 1.6-2.7% in the 0.005-1 MeV neutron energy range. The fission fragments were recorded using a gas scintillation detector in 4π geometry. The energy of neutrons from the reaction $^{7}Li(p,n)$ was calculated using the time-of-flight method. The masses of the ^{233}U and ^{235}U layers were determined by comparing their alpha activity levels with the alpha activity levels of calibrated layers. The ^{233}U layer contained 11.25% ^{238}U.

Gwin et al. [39] have measured the cross-section for ^{233}U fission by 5-200 keV neutrons. The neutrons were produced by a linear electron accelerator. A boron counter was used to determine the energy dependence of the neutron flux. An ionization chamber was used to record the fission fragments. The data were normalized to the resonance integral in the 22.6-101.3 eV region [20]. The uncertainty of such normalization was 5%.

Zhuravlev et al. [66] have measured the ratio of the cross-sections for ^{233}U and ^{235}U fission by filtered beams of reactor neutrons at 2.24, 55 and 144 keV. An ionization chamber was used to record the fission fragments. The ^{235}U fission cross-section was measured using this technique [67], with normalization to the ^{235}U fission cross-section value at thermal σ°_{f} [34]. The ^{233}U fission cross-section values can therefore be regarded as normalized to σ°_{f} ^{235}U. The σ°_{f} ^{233}U value, which was obtained relative to σ°_{f} ^{235}U, is in good agreement with the recommendation given in Ref. [27].

Zhagrov et al. [68] have measured the ^{233}U fission cross-section for incident neutron energies of (44 + 7) keV and (120 $\pm$ 9) keV. The neutron flux was determined relative to the reaction Mn(n,γ) from β and γ coincidences. Mica detectors were used to record the fission fragments. No information is given about the calibration of the layer. The error level for the cross-section was 4%.

Mostovaya et al. [40] have measured the ^{233}U fission cross-section in the 0.1-100 keV neutron energy region. A linear electron accelerator was used as neutron source. The reaction $^{10}B(n,\alpha)$ was used in determining the energy dependence of the neutron flux. An ionization chamber with a high time resolution was used to record the fission fragments. The measurement results were normalized in the 166.9-1223.3 eV region to a resonance integral taken from Ref. [39].

Using a neutron spectrometer based on neutron moderation in lead, Bergman et al. [41] have measured the ^{233}U fission cross-section and its relation to the ^{235}U fission cross-section in the 0.2-50 keV range. The neutron flux was determined relative to

the reaction $^{10}B(n,\alpha)$. An ionization chamber was used to record the fission fragments. The thermal calibration method was used to convert the data to absolute values. The error level for the cross-section was 0.7-2.1%, while that for the ratio was 0.8-2.3%.

3.2. Analysis of the experimental data and evaluation of the $\sigma f(233U)$ energy dependence

From even a cursory analysis of the experimental data it is possible to conclude that the levels of accuracy claimed in the references cited above do not correspond to the systematic differences between the data produced by the various authors. Performing measurements for ^{233}U is a complex task owing to the way its high alpha activity level affects fission fragment recording efficiency and to the sometimes low isotopic purity of the layers (the correction for the presence of other isotopes can be as high as ~3%). However, no clear correlation can be identified between, on the one hand, the differences in the ratio measurements in terms of shape or absolute value and, on the other hand, the method used to determine the recording efficiency ratios and the numbers of nuclei in the ^{233}U and ^{235}U layers. The results of absolute fission cross-section measurements are an important addition to the experimental data. Therefore, using the ^{235}U fission cross-section from ENDF/B-VI [69], we move from the ^{233}U and ^{235}U fission cross-section ratios to σ_f ^{233}U. The σ_f ^{235}U evaluation given in ENDF/B-VI takes into account all the main characteristics of the energy dependence of the fission cross-section found in the latest experimental work [70].

From the totality of the data for neutrons with energies greater than 0.1 MeV, it is possible to single out some groups of data which correspond to the different tendencies in the behavior of the fission cross-section. Carlson's data [49] form the core of the first of these data groups. The results obtained by Fursov et al. [57], Shpak et al. [59], White et al. [61], Pfletchinger et al. [63] and Iyer [54], the results of the absolute measurements performed by Kalinin et al. [52] and the data obtained at the Radium Institute and the Technical University in Dresden [50] agree by and large with Carlson's data. The data obtained by Meadows [55, 56] and Kanda et al. [58]

and the results of the absolute measurements at 14.62 MeV performed by Zasdany et al. [51] belong to the second group. It is reasonable to say that the data in Refs [51, 55, 56] are systematically higher than the data in the first group, while the results in Ref. [58] for measurements in the region of the fission neutron spectrum maximum (~2 MeV) are higher than the data in both groups and have a significantly different shape. Poenitz's absolute measurement results [53] are somewhat dispersed, but on the whole they agree better with the data in the first group.

Let us now look at the data in detail. The largest discrepancies(~10%) are observed near 300 keV. Ref. [57] gives the lowest level and Ref. [53] the highest. The situation is complicated by the fact that, according to all sources except Ref. [59], the cross-section here has a non-monotonic resonance-like character; in Ref. [59], owing to the poor resolution, there is only a "step" in the cross-section in the 200-400 keV energy region. The evaluated curve in the 0.1-0.4 MeV range is based on the data in Ref. [49]. In the 0.4-2.0 MeV region, the results of Refs [57] and [49] are in good agreement. In the 0.55-0.85 MeV range there is another "step" in all the data series. The third such irregularity occurs in the 1.2-1.5 MeV region. The results in Ref. [55] for the 0.4-2.0 MeV region are systematically higher than the data in the first group, but they reproduce both the "steps" noted in Refs [49] and [57]. The results in Ref. [58] have a comparatively large spread in this region and are systematically higher than the data in Ref. [55]. The evaluated curve in the 0.4-2 MeV region is based on the data in Refs [49] and [57] (Fig. 3.2).

In the neutron energy region between 2 MeV and the (n,n'f) reaction threshold (Fig. 3.3), Ref. [58] gives the highest fission cross-section level. The results in Ref. [55] for the 1.5-3 MeV range have an energy dependence different from that of the data in Ref. [58]; they are 2-3% lower than them and systematically higher than the data in the first group. Ref. [57] contains the most detailed study of this neutron energy range. The data of Nesterov et al. [62] have a comparatively large dispersion and are not shown in Fig. 3.3, but on the whole they agree more with the results in Ref. [57]. The data in

Ref. [49] are in good agreement with the data in Ref. [57] as regards both the shape of the energy dependence and absolute value. The other data series [53, 55, 58] have differing energy dependencies in this region, while the absolute differences are as high as ~7%.

Thus, in the 2.0-3.5 MeV energy range the evaluated curve is based on the data in Refs [49] and [57] and agrees with Refs [52] and [61]. In the 3.5-5.5 MeV region, the evaluated cross-section is determined by averaging the data in Refs [49] and [57], owing to the minor (< 1%) difference between them (Fig 3.3).

Near the (n,n'f) reaction threshold and the second "plateau" between 5.5 MeV and 7.4 MeV, the evaluation was based on the data in Refs [49] and [57], the "break" in the energy dependence of the values in Ref. [49] near 7 MeV being ignored. It should be noted that from the (n,n'f) reaction threshold to where the cross-section reaches the second "plateau" data in the first and second groups are in fairly good agreement, but that over a wider range the fission cross-section energy dependencies derived from the data in the two groups and in Ref. [53] differ. This shows up clearly at energies above 8.0 MeV, where the data in Refs [55, 56] give a σ_f level which is approximately 5% higher than the values in the first group. In the 7.4-20 MeV region, the evaluated curve is based on the data in Ref. [49] and agrees with the data in Refs [50, 54, 61] (Fig. 3.4). At neutron energies below 100 keV, the ^{235}U fission cross-section is not a smooth function of the incident neutron energy and is not regarded as a standard cross-section. We therefore looked at two types of work in the case of this region: (1) work where the ratio of the ^{233}U and ^{235}U fission cross-sections is measured; 2) work where the ^{233}U fission cross-section is normalized to the thermal cross-section or the resonance integral of the ^{235}U fission cross-section.

In the 10-100 keV neutron energy region, the results of direct measurements of the ^{233}U fission cross-sections were renormalized to Deruytter's fission integral [17] (data from Refs [39] and [40]); the results given in Refs [41] and [66] were renormalized to the ^{233}U and ^{235}U thermal fission ross-section [27]. The data for the neutron energy region below 40 keV were analyzed in the preceding chapter, and we therefore

consider only the 40-100 keV range here. The data in Refs [39] and [41] are in good agreement, but within the error limits they also agree with the results given in Refs [66] and [68], which are systematically about 5% lower than the data in Ref. [39] (this is a mistake in normalizing to Weston's resonance integral [20] in the 22.6-101.3 eV range). The energy dependencies of the data in Refs [39] and [40] are in agreement. However, in view of the fact that the results of the relative measurements of the ^{233}U and ^{235}U fission cross-sections in Refs [49] and [57] agree more closely with the ratio of the average ^{233}U and ^{235}U cross-sections given in Ref. [39] than with the data in Ref. [40], we give preference to the data in

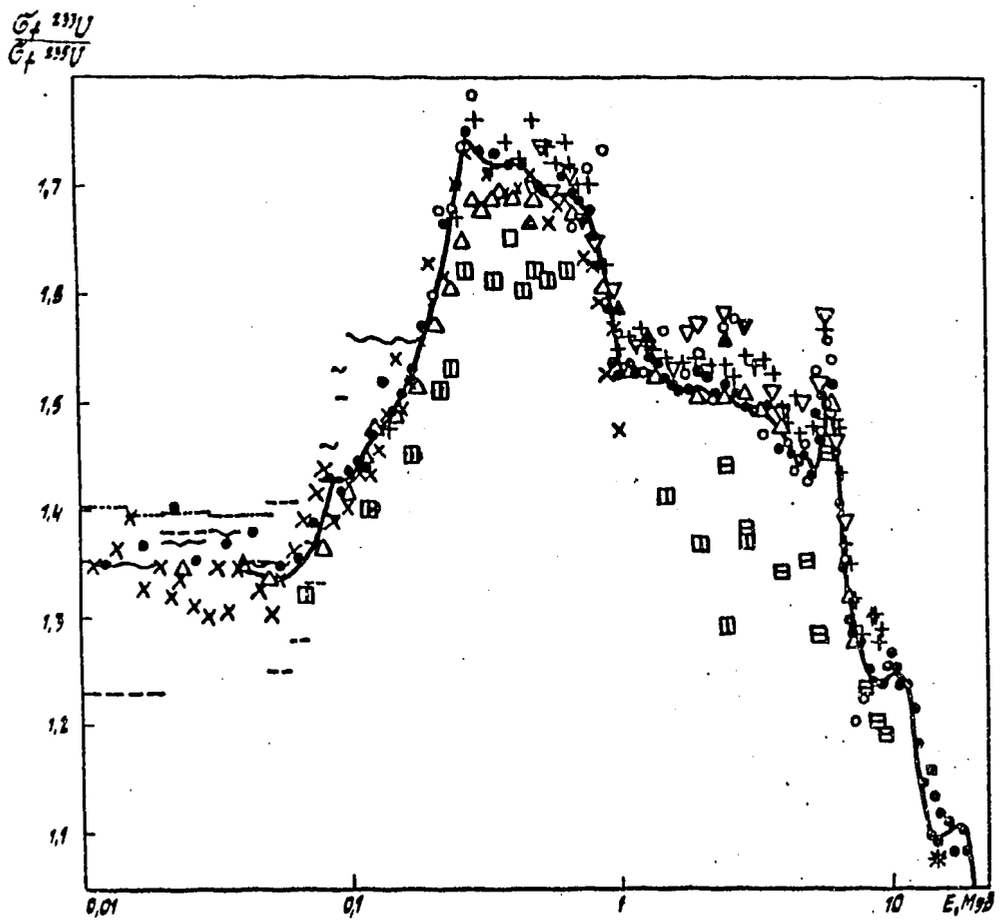

Fig. 3.1: $^{233}U/^{235}U$ fission cross-section ratios:

- evaluated fission cross-section ratio ———
- experimental data: Ref.39 ~ ; Ref.40 - - - ; Ref.41 ——— ; Ref.49 ● ; Ref.50 ★ ; Ref. 53 O ; Ref.55 + ; Ref.57 Δ ; Ref.58 ∇; Ref.62 ▲ ; Ref.63 x ; Ref.64 ⊟ ; Ref.65 ⊞ .

Ref. [39] (Fig. 3.5). The ratio of the average ^{233}U and ^{235}U cross-sections given in Ref. [40] is on the whole lower than the totality of the experimental values. Figure 3.1 compares the experimental ^{233}U and ^{235}U fission cross-section ratios and the evaluated curve which was obtained using the evaluated ^{233}U fission cross-section and the ^{235}U fission cross-section given in ENDF/B-VI. The evaluated curve reflects the main characteristics of the energy dependence of the ^{233}U and ^{235}U fission cross-section ratio. The most pronounced peak at $\nu = 6$ MeV is caused by the difference in the (n,n'f) reaction thresholds for the neutron fission of ^{233}U and ^{235}U.

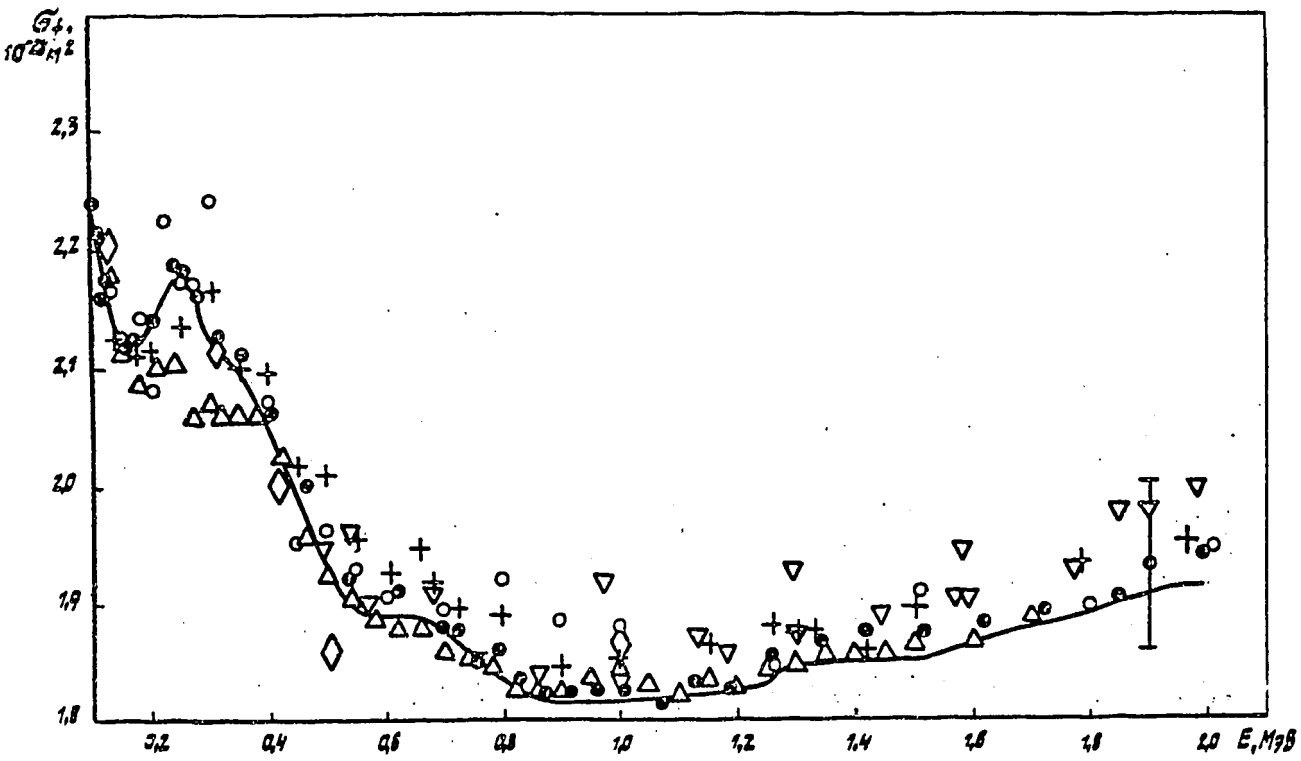

Fig. 3.2: ^{233}U fission cross-section for 1-2 MeV neutrons:
- evaluated fission cross-section ———
- experimental data, Ref.52 ◐ ; Refs.60,61 ◇ ;
(see Fig. 1 for other reference symbols)

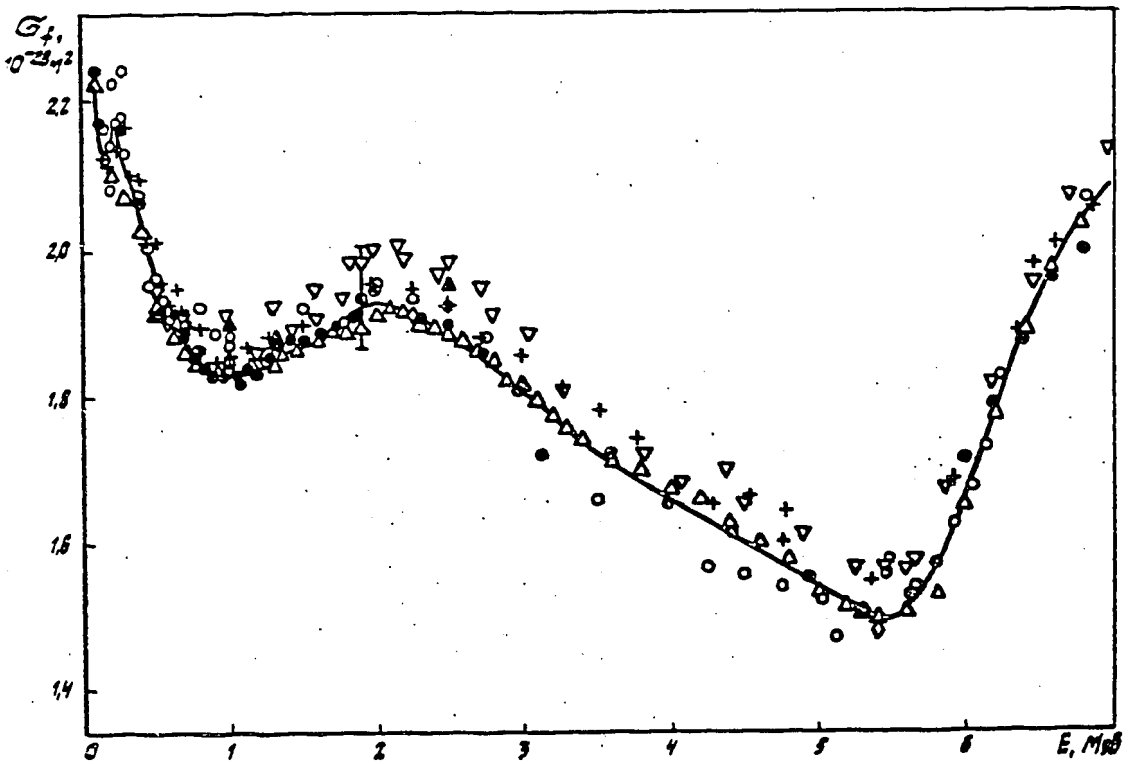

Fig. 3.3: ^{233}U fission cross-section for 0.1-7 MeV neutrons (see Figs. 3.1 and 3.2 for reference symbols)

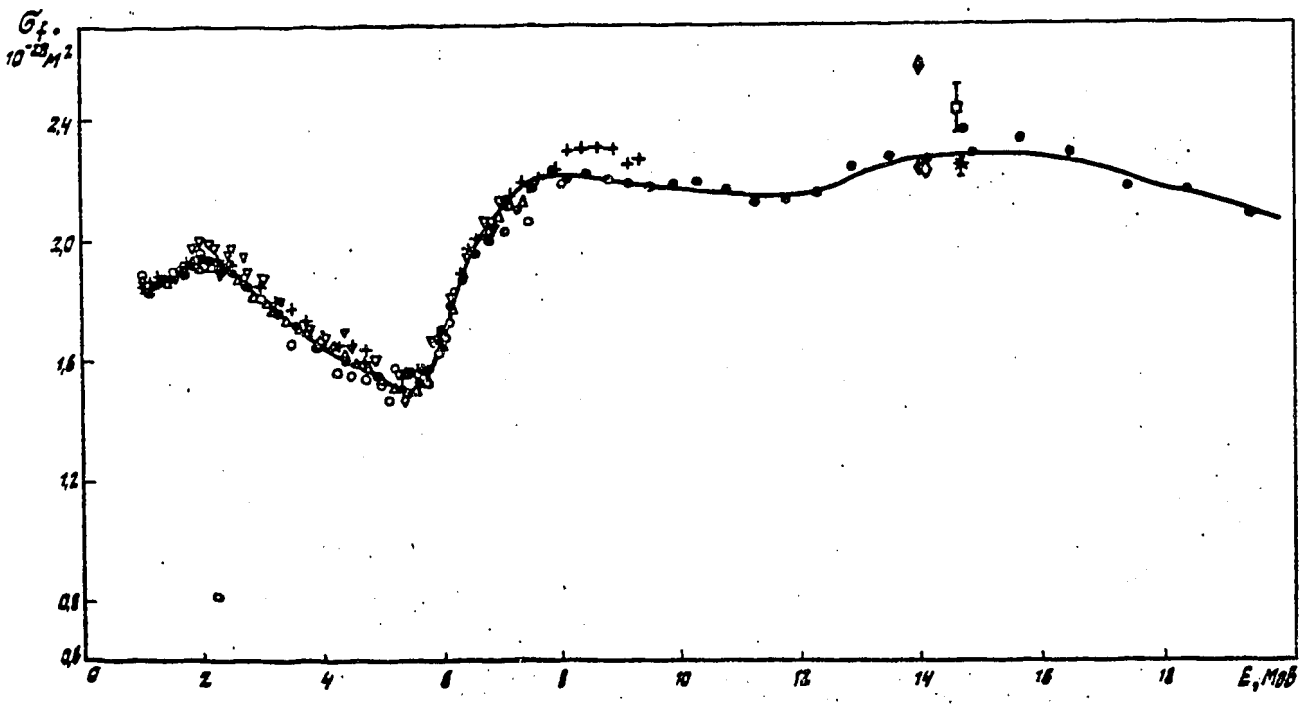

Fig. 3.4: ^{233}U fission cross-section for 1-20 MeV neutrons: Ref.51 ■ ; Ref.54 ♦ ; Ref.56 ⊗ ; (see Figs 3.1 and 3.2 for reference symbols)

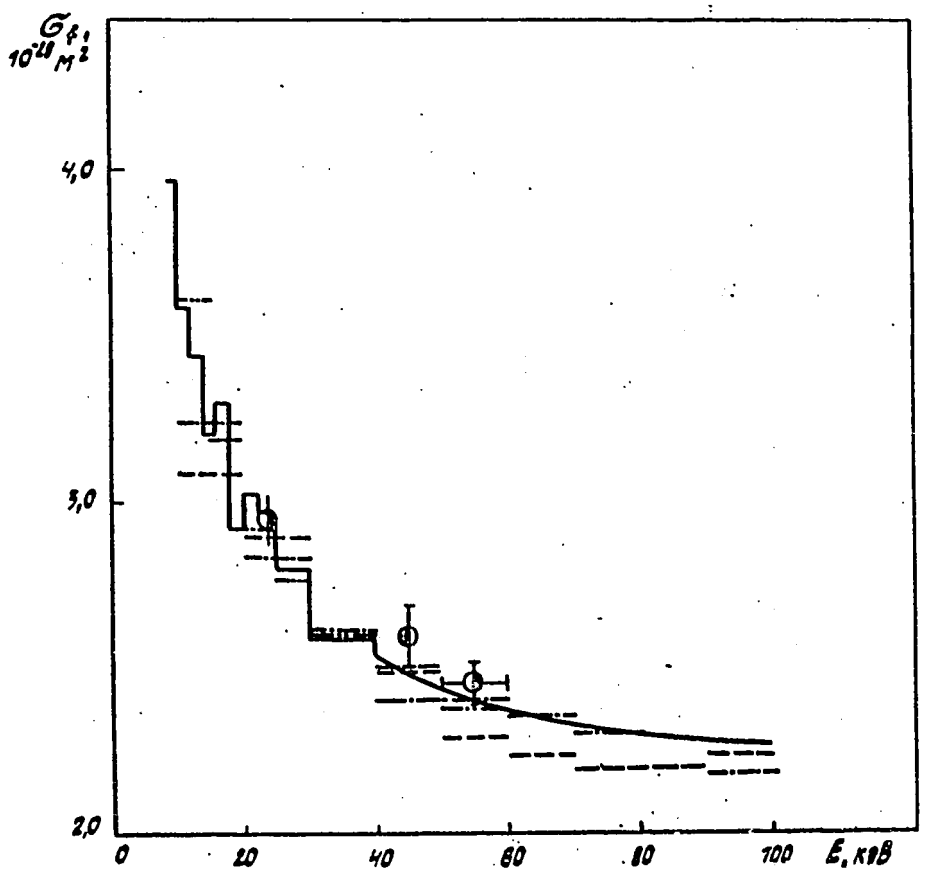

Fig. 3.5: ^{233}U fission cross-section for 1-100 keV:
evaluated data ———
experimental data: Ref.38 —·—·; Ref.40
Ref.41 —··—··—; Refs 66,67 ●; Ref.68 ●

4. CROSS-SECTIONS FOR THE INTERACTION OF NEUTRONS WITH THE ^{233}U NUCLEUS IN THE FAST NEUTRON ENERGY RANGE 0.04-20 MEV

Experimental cross-section data for the interaction of fast neutrons with the ^{233}U nucleus, excluding fission cross-section measurements described in the previous chapter, make it possible determine fairly reliably the total interaction cross-section. Furthermore, data on measurements of α in the energy range up to 1 MeV and elastic and inelastic scattering cross-sections at the first levels at several energy points below 3.5 MeV can be used in the evaluation.

4.1. Evaluation of total cross-section

There are six sets of experimental data on $\sigma_t(^{233}U)$, each of which partially covers the 0.04-20 MeV energy range:

- Stupegia [71] for incident neutron energies of 3.4-1611 keV with an error of ν 2.5%;
- Foster et al. [72] in the energy range 2.5-15 MeV with an error of ν 1-2%;
- Green et al. [72] in the neutron energy range 0.5-10 MeV with considerable error;
- Poenitz et al. [37] for $0.04 \leq E_n \leq 4.43$ MeV with an error of 1.5 to 4%
- Ponitz et al. [74] in the energy range 0.03-4.8 MeV with an error of 2-2.5%;
- Poenitz et al. [75] for neutron energies of 1.8-20 MeV with an error of 1.5-2%.

The data in Ref. [71] are systematically lower than all the others and the results in Ref. [73] have a significant spread. The evaluated curve for $\sigma_t(E)$ in the region up to 12 MeV was constructed using the least squares method without taking into account the data in Ref. [71]. Weights of all the remaining experimental data were assigned which were inversely proportional to the square of their errors.

The dependence $\sigma_t(E)$ thus obtained is described in the framework of the coupled channel method with the potential parameters calculated earlier for actinides [76] by varying only the deformation parameters β_2 and β_4. The difference between the evaluated and calculated curve does not exceed 2% over the whole energy range, and therefore in evaluating σ_t at $E_n > 12$ MeV, for which we have experimental data only from one work, we took into account the energy dependence predicted by the calculation.

4.2. Optical cross-sections

The optical cross-sections and the neutron transparencies necessary for the statistical calculations were obtained by the least squares method using the potential parameters [76]:

$$V_R = (46{,}14 - 0{,}3\,E)\ \text{МэВ}, \qquad r_R = 1{,}256\ \text{Фм}, \quad a_R = 0{,}626\ \text{Фм},$$

$$W_D = \begin{cases} (3{,}12 + 0{,}4\,E)\ \text{МэВ} & (E \leq 10\ \text{МэВ}), \\ 7{,}12\ \text{МэВ} & (E > 10\ \text{МэВ}), \end{cases} \qquad \begin{aligned} r_D &= 1{,}26\ \text{Фм}, \\ a_D &= (0{,}555 + 0{,}0045\,E)\ \text{Фм}, \end{aligned}$$

$$\beta_2 = 0{,}186, \quad \beta_4 = 0{,}090.$$

The deformation parameters β_2 and β_4 were refined by fitting to the evaluated curve of $\sigma_t(E)$, as noted above, and to the values of the strength function S_0 and the potential scattering radius R' evaluated in the resonance region. The values for S_0 and R' obtained by calculations with the given potential

parameters were 0.995 x $10^{-4}(eV)^{-1/2}$ and 9.51 fm respectively. The calculations were performed taking into account the link between the first five levels of the main rotational band of the ^{233}U nucleus (Table 4.1). The quality of the description of the total cross-section σ_t is shown in Fig 4.1.

4.3. Calculations using the statistical model

For neutrons with energies below the threshold of the (n,n'f) reaction, the cross-sections of the σ_{nx} reactions - fission (n,f), radiative capture (n,γ) and the (n,n') reaction - were calculated using the statistical theory of nuclear reactions:

$$\sigma_{nx} = \frac{\pi\lambda^2}{2(2I+1)} \cdot \sum_{J\ell j} (2J+1) \cdot T_{\ell j}^{J\pi} \cdot P_x^{J\pi} \cdot S_{nx}^{J\pi\ell j} \quad ;$$

$$P_x^{J\pi} = \frac{T_x^{J\pi}(U)}{T_n^{J\pi}(U) + T_{n'}^{J\pi}(U) + T_\gamma^{J\pi}(U) + T_f^{J\pi}(U)} \, ,$$

where U = B_n + E is the excitation energy of the compound ^{234}U nucleus ; B_n is the separation energy of the neutron from ^{234}U; $T_{lj}^{J\pi}$ are the neutron attachment factors calculated using the coupled channel method with the deformation potential given above; $P_x^{j\pi}$ is the probability of the (n,x) reaction in the $[J^{\pi}_{lj})$ channel determined by the transparency ratio of elastic T_n and inelastic $T_{n'}$ scattering and also of the radiation T_γ and fission T_f channels; $S_{nx}^{j\pi lj}$ is the factor taking into account partial width fluctuations.

The transparency of the inelastic scattering channel $T_{n'}$ is determined by the ratio

$$T_{n'}(U) = \sum_{\ell' j' I'} \tilde{T}_{\ell' j'}^{J\pi}(E') \cdot \rho_n(U - B_n - E', I', \pi') \, dE' ,$$

whereby the emitted neutron transparencies $\tilde{T}_{l'j'}^{J\pi}(E')$ were calculated using the spherical optical potential, which reproduces well the cross-section for the formation of the compound ^{234}U nucleus calculated by the coupled channel method [78]; $\rho_n(U-B_n-E',I',\pi')$ is the ^{233}U compound nucleus level density.

The level density $\rho(U,J,\pi)$ was calculated using the phenomenological model taking into account shell, superfluid and collective effects [45]:

$$\rho(U,J,\pi) = K_{rot}(U,J) \cdot K_{vib}(U) \cdot \rho_{nqp}(U,J,\pi),$$

where $\rho_{nqp}(U,J,\pi)$ is the level density with spin J and parity π in the non-interacting quasi-particle model.

Factorization of the contribution of the collective rotational excitation $K_{rot}(U,J)$ and vibrational excitation $K_{vib}(U)$ to the total level density corresponds to their adiabatic separation. Shell effects on level density were modelled by introducing the energy dependence of the main level density parameter:

$$a_{n(f)}(U) = \begin{cases} \tilde{a}_{n(f)} \left\{1 + \delta W_{n(f)} \frac{f(U - E_{конд})}{U - E_{конд}}\right\}, & U > 0{,}47\, a_{n(f)} \cdot \Delta^2_{n(f)} - m \cdot \Delta_{n(f)}; \\ a_{n(f)}(U_{кр}) = a_{кр}, & U < 0{,}47\, a_{кр} \Delta^2_{n(f)} - m \cdot \Delta_{n(f)}, \end{cases}$$

where m = 0, 1, 2 - for even-even, odd-even(even-odd) and odd-odd nuclei respectively; $f(x) = 1-\exp(-\gamma x)$ is the dimensionless function defining the energy changes caused by the shell effects.

In order to calculate the corrections for the shell effects δY_n for the purpose of calculating the level density of the residual nucleus, we used experimental values for the nuclear masses [6] and the parameters of the Myers-Swiatecki liquid drop model [79]. The correlation functions Δ_n were determined from the even-odd differences in the nuclear binding energy.

At low excitation energies $U < U_c = 10.7 - 0.028\, A - m\Delta_{o(f)}$, where A is the mass number, the total level density $\rho(U)$ was modelled by the simple temperature dependence in the well-known Gilbert-Cameron approach. This procedure can be regarded as a renormalization of the results of the superfluid model at low excitation energies, making it possible to reproduce the increasing contributions of low-lying levels:

$$\rho(U) = \exp[(U + m\Delta)/T];$$

$$T = \left\{\frac{d}{dU}\left[\ln \hat{\rho}(U)\right]\Big|_{U=U_c}\right\}^{-1};$$

$$\hat{\rho}(U) = \frac{K_{рот} \cdot K_{кол}}{\sqrt{2\pi}\, \sigma_{\parallel}} W_{нкч}(U),$$

where $\sigma_\parallel$ is the parallel moment of spin dependence $\rho(U,J,\pi)$; W_{nqp} is the density of internal quasi-particle excitations [45].

The value of U_c is the point at which the superfluid model and the constant temperature model join. By systematizing the parameters U_c and T we obtained D_{obs} = 0.34 eV for the compound ^{234}U nucleus which agrees well with the value of 0.42 eV adopted in this work . For ^{233}U the present value for D_{obs} is 3.81 eV, which agrees well with D_{obs} = 4.1 eV [80]. In order to calculate the level densities of the ^{232}U and ^{231}U nuclei formed in the (n,xn) reactions, we used the systematized results of Ref. [81]. For the ^{234}U and ^{233}U nuclei the value of ã was determined by normalizing $\rho(U,J,\pi)$ to the observed neutron resonance density evaluated in this work and in Ref. [80] respectively.

The radiation transparencies $T_\gamma^{J\pi}$ were calculated using the Axel-Brink approximation [82] assuming that the main contribution to γ emission is made by the electric dipole gamma transitions:

$$T_\gamma^{J\pi} = \frac{1}{3}\frac{c_\gamma}{(\pi\hbar c)^2}\int_0^U \varepsilon_\gamma^2\sigma_\gamma^2(\varepsilon_\gamma)\sum_{J=|I-1|}^{I+1}\rho(U-\varepsilon_\gamma,I)\,d\varepsilon_\gamma .$$

In order to calculate the photoabsorption cross-section $\sigma_\gamma(\epsilon_\gamma)$, $\epsilon_\gamma \leq U$ the parametrization in Ref. [83] was used, taking into account splitting of giant dipole resonance for actinides and making a good approximation of $\sigma_\gamma(\epsilon_\gamma)$ for low energy γ quanta:

$$\sigma_\gamma(\varepsilon_\gamma) = \sum_{i=1}^{2}\sigma_i\frac{\varepsilon_\gamma^2\Gamma_{\sigma i}^2}{(\varepsilon_\gamma^2-E_{\sigma i}^2)^2+\varepsilon_\gamma^2\Gamma_{\sigma i}^2};$$

σ_1 = 250 mb, $E_{\sigma 1}$ = 10.5 MeV, $\Gamma_{\sigma 1}$ = 2.5 MeV,
σ_2 - 300 mb, $E_{\sigma 2}$ = 14 MeV, $\Gamma_{\sigma 2}$ = 4.5 MeV.

The constant c_γ was determined by the normalization of the radiative capture widths

$$\langle \Gamma_{\gamma c}^{J\pi}(B_n)\rangle = -\frac{T_{\gamma\gamma}^{J\pi}(B_n)}{2\pi\rho(B_n,J,\pi)}$$

to the observed value of the total radiation width $\langle\Gamma_\gamma\rangle$ = 39 MeV and was found to be 1.21. The neutron radiative capture transparency $T_{\gamma\gamma}^{J\pi}(B_n)$ was calculated by taking into account the competing (n,$\gamma\gamma$), (n,γn') and (n,γf) reactions [84].

In the double-humped barrier model [85], the neutron fission N of odd actinides can be considered a two-stage process consisting of consecutive transmission through the internal A and external B thresholds. In this case, the transparency of the fission channel $T_f^{J\pi}(U)$ can be represented as

$$T_f^{J\pi}(U) = T_{fA}^{J\pi} \cdot T_{fB}^{J\pi} / (T_{fA}^{J\pi} + T_{fB}^{J\pi})$$

The fission transparency of each of the humps is determined by the level density in the transitional state $\rho_x(\epsilon, J, \Pi)$ at the corresponding deformation:

$$T_{fx}^{J\pi} = \sum_K T_{fxK}^{J\pi} + \int_0^U \left\{1 + \exp\left[\frac{2\pi}{\hbar\omega_x}(E_f^x + \varepsilon - U)\right]\right\}^{-1} \cdot \rho_x(\varepsilon, J, \pi)\, d\varepsilon,$$

where E^x_f and hW_x is the height and curvature of the barrier $x = A(B)$.

For the even-even fissile nucleus (^{234}U) at neutron energies of $E \leq U_2 + E_f^{A(B)} - B_n$, i.e. below the two-quasi particle state excitation threshold, $T^{J\Pi}_{fxk}$ was determined by the collective levels in the energy gap. The collective level spectra for the internal and external saddle configurations of light uranium isotopes are different. They are associated with the asymmetry of the saddle configurations. The internal saddle of the uranium nucleus with $A \leq 234$ is stable with respect to γ deformations, but the external saddle configuration has mass asymmetry, whereby $E^A_f < E^B_f$ [86]. As a result, $K^A_{rot} \sim \sigma_\perp^2$ and $K^B_{rot} \sim 2 \cdot \sigma^2_\perp$. Moreover, in view of the mass asymmetry of the external saddle configuration, the collective states of bands with negative parity $K^\Pi = 0^-, 1^-, 2^-, 3^-$ are significantly lower than the corresponding states in the nucleus with small quadrupole deformation. For the internal saddle, the values of $E_{k\pi}$ for the ^{234}U nucleus [77] were taken as the band foundation positions and for the outer saddle, the values in Ref. [87] were taken as an initial approximation. After that they varied slightly. In order to construct the complete scheme of transitional states, the band foundations were supplemented by rotation bands with the following energies :

$$E_{JK\pi} = E_{K\pi} + \frac{\hbar^2}{2F_\perp^{A(B)}}\left[J(J+1) - K(K+1)\right];$$

$$\hbar^2/2F_\perp^A = 6{,}5 \text{ кэВ}; \quad \hbar^2/2F_\perp^B = 2{,}5 \text{ кэВ}.$$

In addition to the $E_f^{A(B)}$ fission barriers, the other parameters of the model were the shell corrections $\delta W_f^{A(B)}$ and the correlation function of the nucleus in the transitional state Δ_f. The shell corrections, taken from Ref. [81], generally corresponded to the form

$$\delta W_f^{A(B)} = E_f^{A(B)} - E_{NXK}^{A(B)},$$

where $E^{A(B)}$ is the liquid drop forming fission barrier at the corresponding deformations.

The correlation function Δ_f was determined by the energy dependence of σ_f in the 2-5.5 MeV region. The theoretical barriers given in Ref. [86] were taken as the initial values of $E_f^{A(B)}$. The values of E_f^A and E_f^B, which enable us to describe the experimental cross-section data for the $^{233}U(n,f)$ reaction, agree well with the results of the theoretical calculations of the fission barriers [86] (see Ref. [88]). Similar agreement is observed in the case of the compound ^{233}U and ^{232}U nuclei fissioning in the (n,n'f) and (n,2nf) reactions. The fission barrier parameters are given in Table 4.2.

Having established the parameters for the optical potential, level density, fission barriers and radiation strength function, we can proceed to calculate the neutron cross-sections.

Figure 4.2 shows the experimental data from Ref. [89] on angular distributions of elastically and inelastically scattered neutrons. By means of incoherent summation of the cross-sections of direct and compound level excitation, we can obtain a good description of the angular distributions at 1.5 MeV. At 0.7 MeV it is not possible to obtain a satisfactory description of the angular scattering of neutrons which excite level $7/2^+$. Evidently the experimental excitation cross-section for the first level $7/2^+$ is too high by a factor of approximately two. Figure 4.3 shows a comparison of the $7/2^+$(a) and $9/2^+$(b) level excitation cross-sections with data from the JENDL-3 evaluation [90].

Figure 4.4 compares the experimental results from Refs [89 and 91] and the evaluated elastic scattering cross-sections given in JENDL-3, the present work and ENDL-78 [92]. It should be

borne in mind that owing to inadequate resolution, the data in Ref. [91] contain the contribution of inelastically scattered neutrons. The calculated cross-sections for excitation of the first levels for ^{233}U have therefore been subtracted from the values from Ref. [91] given in Fig. 4.4. Despite this, they do not agree satisfactorily with the calculated curve for $\sigma_n(E)$.

The data in Ref. [91] represent the sum of elastic scattering cross-sections and level excitation cross-sections in the range ΔE_x close to the ground state. Table 4.3 compares the data from Ref. [91] with those calculated in the present work. As will be seen, there is very good agreement with the exception of the 1.49 MeV energy point.

There are no results of direct measurements of the (n,γ) reaction cross-sections for ^{233}U in the neutron energy range above 45 keV. Using data for $\alpha = \sigma_\gamma/\sigma_f$ [93 and 94], we can easily obtain σ_γ for ^{233}U . However, the results of Refs [93 and 94] agree in the 0.030-0.0250 MeV neutron energy range, can be used to predict different energy dependences of $\sigma_\gamma(E)$ in the 0.25-1.0 MeV energy range. At the same time, the data in Ref. [94] at ν 0.9 MeV contradict the systematic pattern of the measurements of α [95] for ^{239}Pu and α for ^{233}U, ^{235}U and ^{239}Pu [93]. The systematically higher values of α for ^{235}U over the values of α for ^{233}U will be maintained in the capture cross-sections.

For the above value of the radiation strength function $S_\gamma = 0.928$, we can reproduce fairly well the energy dependence $\sigma_\gamma(E)$ from the data in Ref. [93] (Fig. 4.5). For $E_n \geq 1$ MeV the sharp drop in σ_γ is determined by the intensified competition of the $(n,\gamma n')$ reaction together with the increase in excitation energy. For $E_n \geq 6$ MeV, the main contribution to the capture cross-section is made by the direct neutron capture mechanism. For $E_n > 10$ MeV, the value of $\sigma_{n\gamma}$ is taken to be 1×10^{-31} m^2 [96].

The statistical approach used enables us to describe the observed fission cross-section below the $(n,n'f)$ reaction threshold with an error of not more than 0.05×10^{-28} m^2. The fission cross-section is calculated by taking into account the $(n,\gamma f)$ process. Its contribution $\beta = \sigma_{\gamma f}/\sigma_f$ to the fission

cross-section is small. It increases slightly from ν 3% at E_n = 0.1 keV to ~7% at E_n ~1.5 MeV and then decreases to ~1% at E_n ~5 MeV. The reason for the increase in the contribution of β as the excitation energy increases at $E_n \leq 1.5$ MeV is obvious. Its reduction at $E_n > 1.5$ MeV is caused by competition of the $(n,\gamma n')$ process. It is impossible to reproduce the stepped characteristics in the observed fission cross-section for neutron energies of E_n ~0.2; 0.55; 1.3 MeV. We can relate this structure partially to the stepped structure in the density of the internal states of the even-even fissile nucleus. The excitation threshold of the two quasi-particle state at the external fission barrier is $E_n \approx 0.5$ MeV, and therefore the stepped irregularity at $E_n \approx 0.55$ MeV can be interpreted as a manifestation of the discrete nature of quasi-particle excitation in the fissile ^{234}U nucleus. The nature of the other irregularities is not clear.

Above the threshold of the (n,n'f) reaction, the behavior of the primary fission cross-section σ^1_{nf} should provide a description of the observed fission cross-section for ^{233}U (n,f). The fission characteristics of the residual ^{233}U nucleus which undergoes fission in the (n,n'f) reaction can be established using data for the ^{232}U (n,f) cross-section [97] and the fission characteristics of the residual ^{232}U nucleus which undergoes fission in the (n,2nf) reaction from data for the (^3He,df) reaction cross-section of the [98]. In order to evaluate the behavior of the primary fission cross-section we use the results of the analysis of the cross-sections for (n,f) and (n,xn) reactions and the spectra of the secondary neutrons for the ^{238}U and ^{235}U nuclei [99]. The behavior of the primary fission cross-section σ^1_{nf} is determined by the hard component of the secondary neutron spectrum and the fissionability of the compound ^{234}U nucleus. In the region of high excitations the fissionability is determined by the shell corrections δW^B_f and δW_n. The hard component of the secondary neutron spectrum is established by the description of the (n,xn) reaction for ^{235}U and ^{238}U. For the above determination of the parameters and for that contained in Refs [73, 88, 89], we fission cross-section for ^{233}U (n,f) can be described with an accuracy not worse than ~ 5% in the neutron energy region up to 20 MeV without additional variation of the parameters (Fig. 4.6).

Figure 4.6 also shows the contributions of emission and non-emission fissions to the observed fission cross-section. It should be noted that the most noticeable discrepancy between the theoretical curve and the evaluated dependence $\sigma_f(E)$ occurs above the threshold of the (n,2nf) reaction. However, in this energy region, there is considerable error associated with the fission cross-sections. This error increases owing to the poor reliability of the ^{235}U (n,f) fission cross-section.

Figure 4.7 compares the cross-sections for the (n,2n) and (n,3n) reactions from the JENDL-2 [100] JENDL-3 [90] and ENDL-78 [92] libraries with the present evaluation. The greatest discrepancy with the JENDL evaluations is observed in the case of the ^{233}U (n,2n) ^{232}U reactions. In the JENDL-2 file, the cross-section σ_{n2n} is obtained by normalization of the energy dependence $\sigma_{n,2n}(E)$ to the $\langle\sigma_{n,2n}\rangle_{fiss}$ measurements in the fission spectrum [101]: $\langle\sigma_{n2n}\rangle_{fiss} = 4 \times 10^{-31}$ m^2. Averaging $\sigma_{n,2n}$ over the fission spectrum [102] we obtain 2.9×10^{-31} m^2 for the present evaluation, 3.8×10^{-31} m^2 for JENDL-2 and 1.6×10^{-31} m^2 for JENDL-3. Moreover, the discrepancies may be associated with the errors in describing the observed fission cross-section for ^{233}U(n,f) and differences in evaluating the contribution of emission fission.

The validity of the present evaluation of σ_{n2n} is confirmed by the description within the framework of this approach of the cross-sections of the ^{238}U(n,2n) ^{235}U(n,2n) ^{239}Pu(n,2n) ^{237}Np(n,2n) ^{232}Th(n,2n) ^{238}U(n,3n) and ^{235}U(n,3n) reactions. The evaluated total cross-section for inelastic scattering differs significantly from the JENDL-3 and ENDL-78 evaluations. The discrepancy in the energy region 0.1-3 MeV with the ENDL-78 evaluation is chiefly associated with the taking into account of the direct level excitation of the ground state rotation band and in the region $E_n > 7$ MeV also with the taking into account of pre-equilibrium neutron emission. The discrepancy with the JENDL-3 evaluation at $E_n > 7$ MeV and the growth of the $\sigma_{n'}$ cross-section at $E_n > 15$ MeV in JENDL-3 are very difficult to explain.

Figure 4.8 shows the experimental values obtained from the data in Refs [37 and 91] for the total cross-section and the

total scattering cross-section, and also the cross-section for fission, capture and first-level excitation evaluated in the present work. Unfortunately, these data do not enable us to give preference to any of the evaluations of $\sigma_{n'}$. The evaluated cross-sections for interaction of fast neutrons with the ^{233}U nucleus are shown in Tables 4.4 and 4.5.

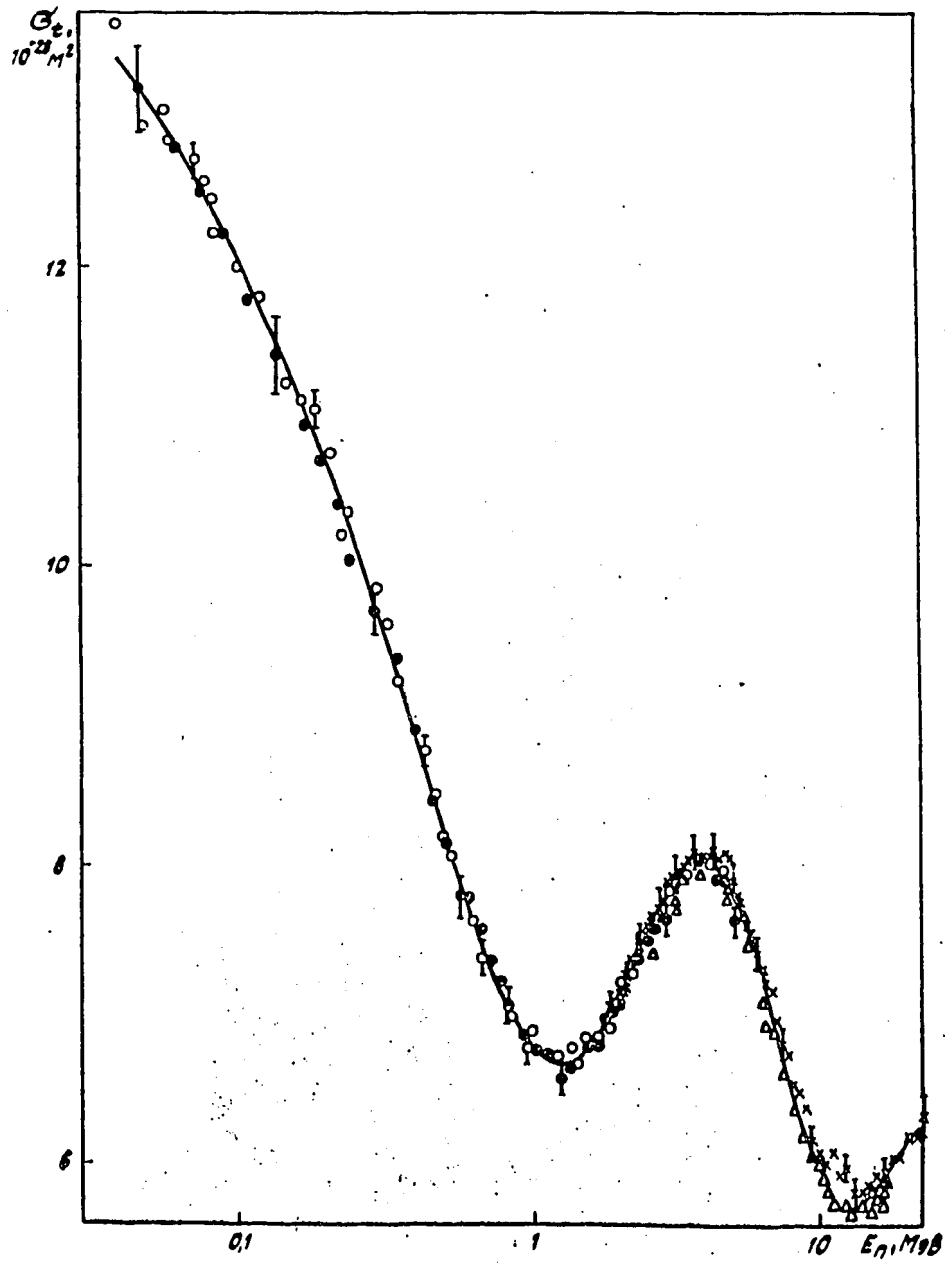

Fig. 4.1 Total interaction cross-section of 0.04-20 MeV neutrons with the ^{233}U nucleus.
The present evaluation ————
Experimental data: Ref.37 O ; Ref.72 Δ ;
Ref.74 ● ; Ref.75 x .

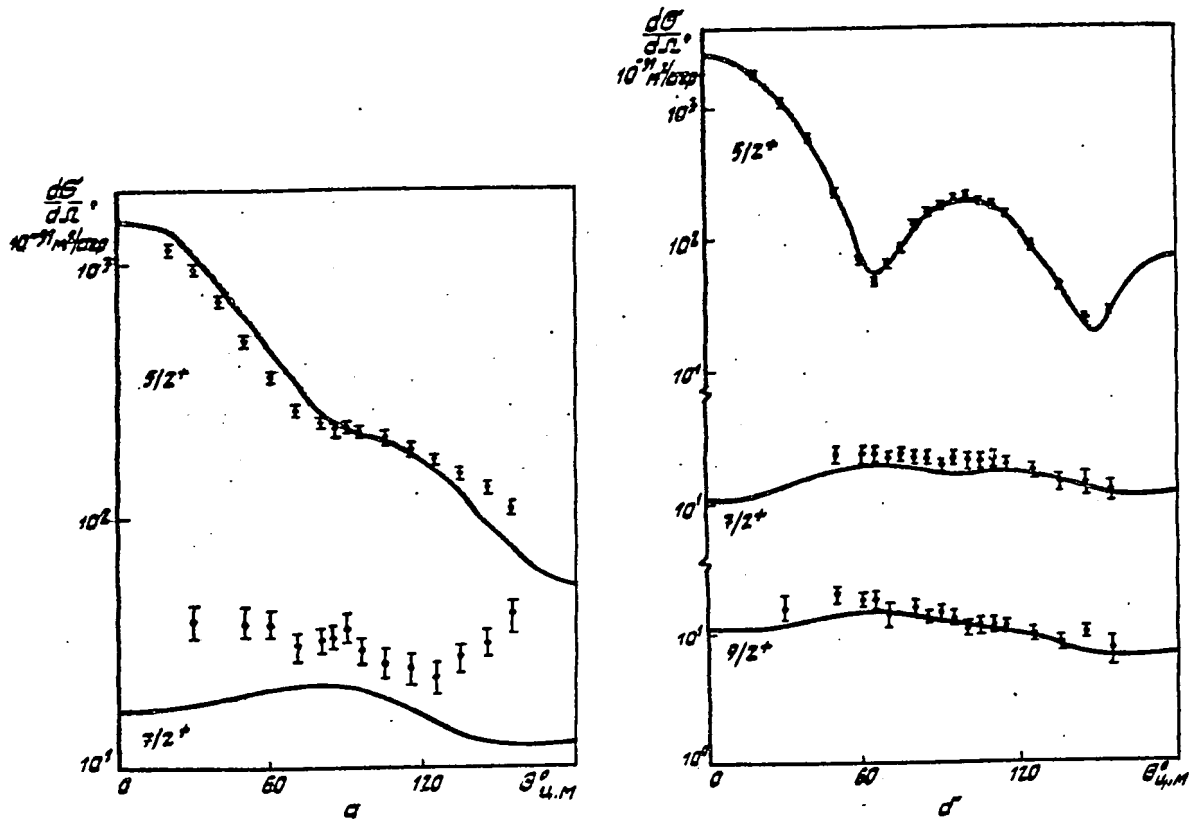

Fig. 4.2 Differential cross-sections for elastic and inelastic scattering of ^{233}U neutrons.
(a) E_n = 0.7 MeV (b) E_n = 1.5 Mev;
——— calculation; Ref.89 data ●

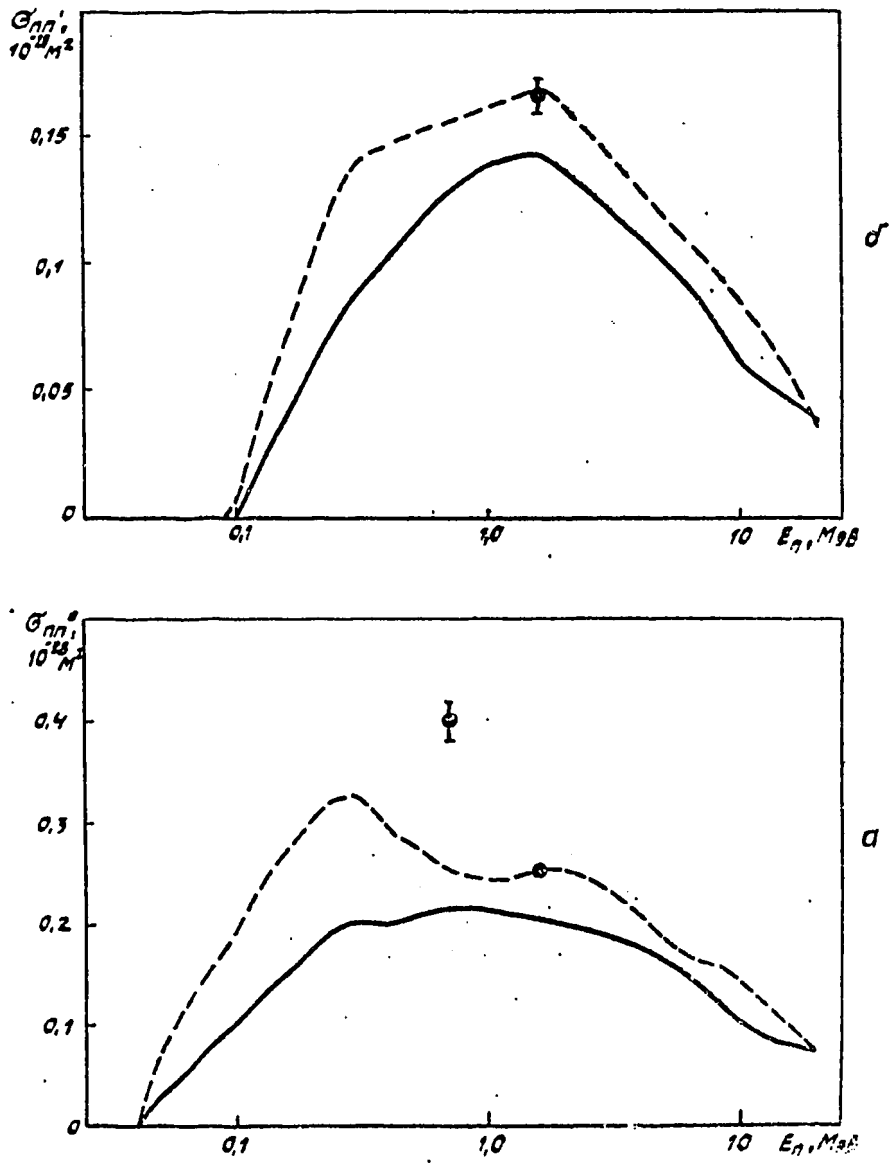

Fig. 4.3 Excitation cross-sections for levels 7/2⁺(a) and 9/2⁺(b); _____ present work; Ref.90 - - - JENDL-3 evaluation ; Ref.89 data ●

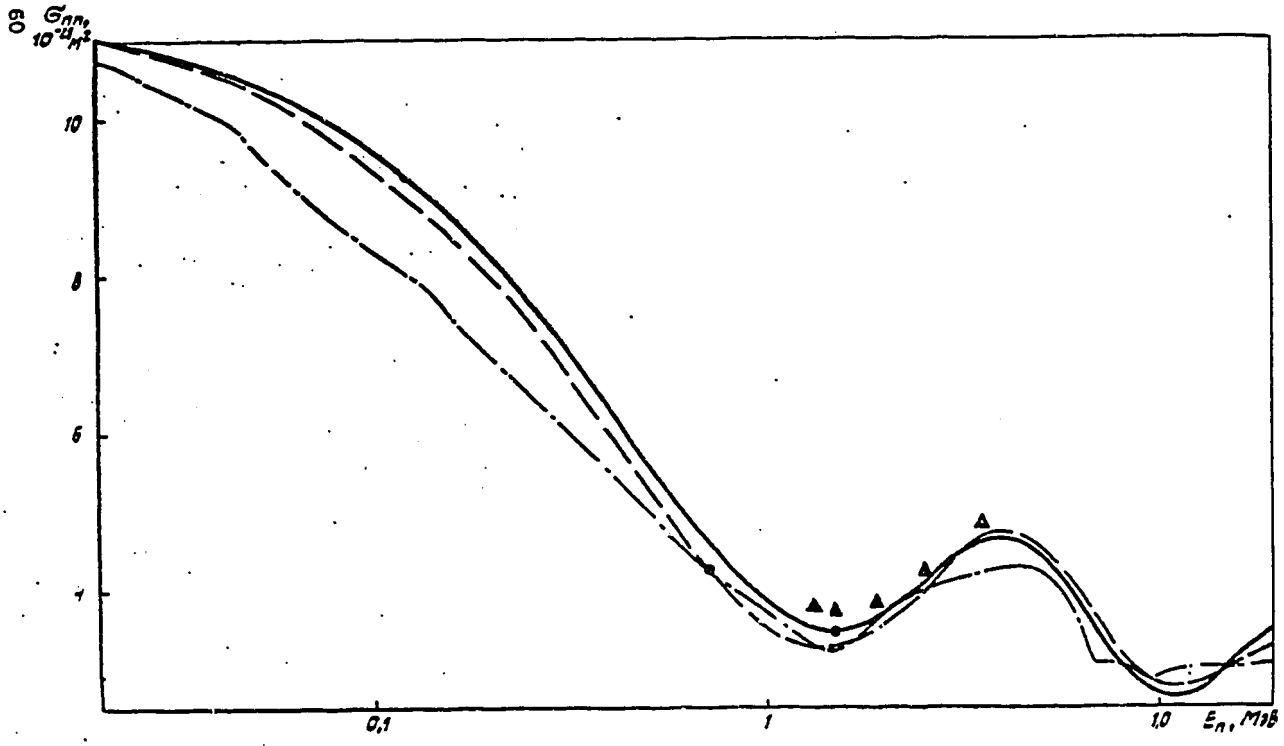

Fig. 4.4 ^{233}U neutron inelastic scattering cross-section.
Present evaluation _____ ; JENDL-3 evaluation - - - - Ref.90; -.-.-. ENDL evaluation Ref.92 ;
Ref.89 experimental data ● ; Ref.91 data ▲ .

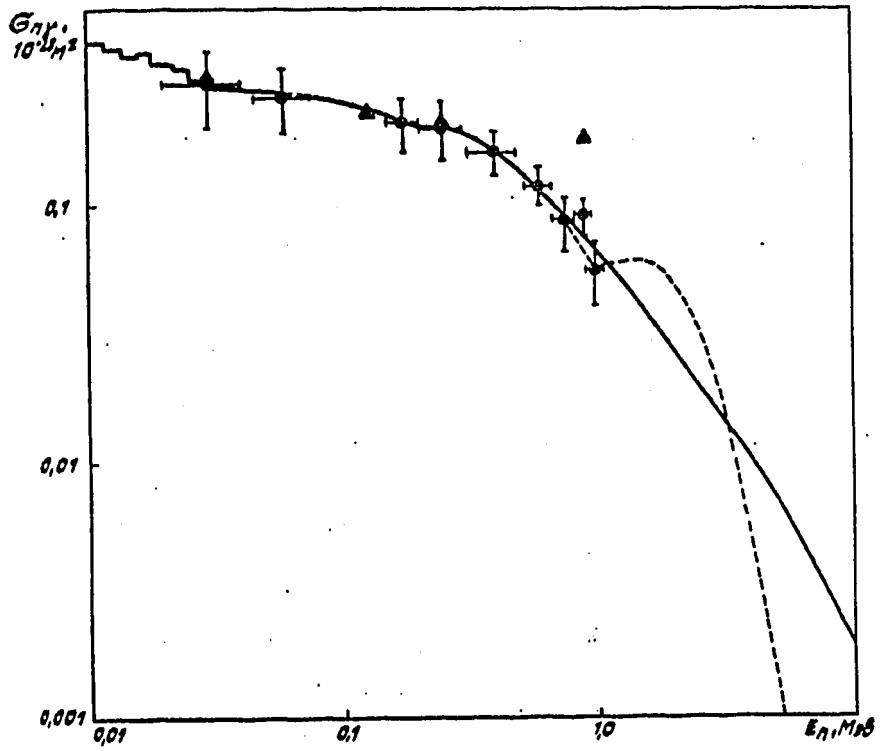

Fig. 4.5 ^{233}U neutron radiative capture cross-section
Present evaluation _____ ;
JENDL evaluation - - - - Ref.90;
● experimental data Ref. 93; ▲ Ref.94.

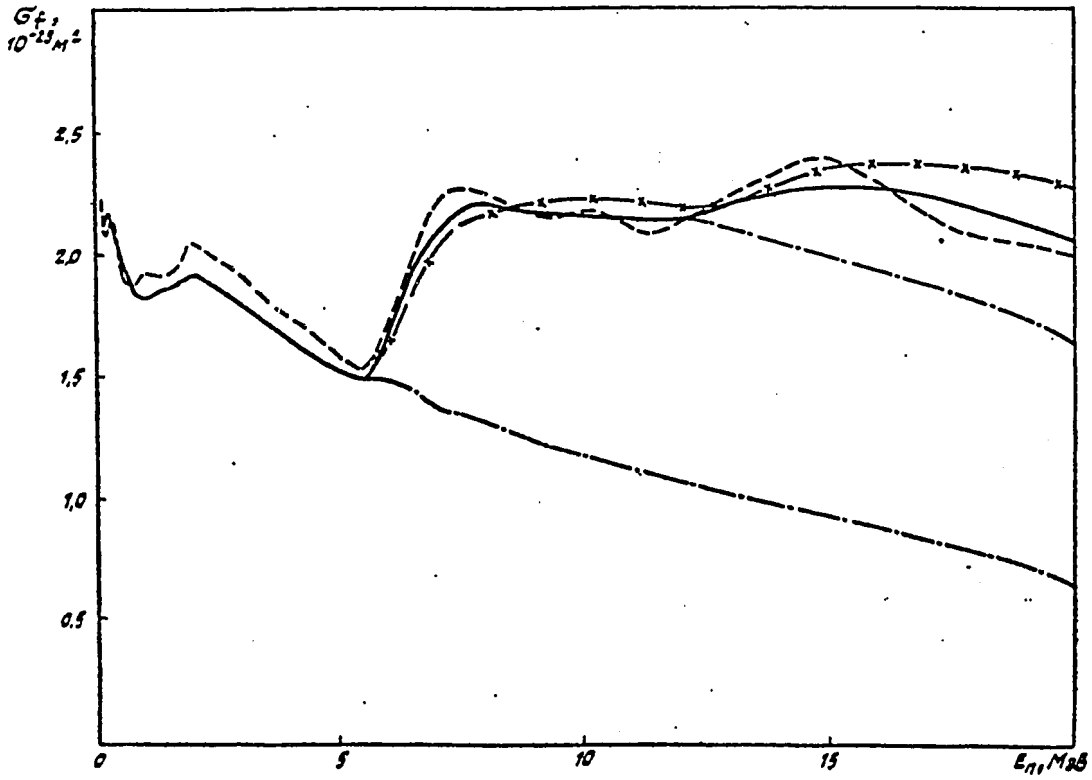

Fig. 4.6 ^{233}U fission cross-section for 1-20 MeV neutrons. Present evaluation _____ ; ____ _ ____ _ contributions to the total fission cross-section of non-emission and emission fissions; - - - - JENDL-3 evaluations [90]; __ x __ x ___ this calculation.

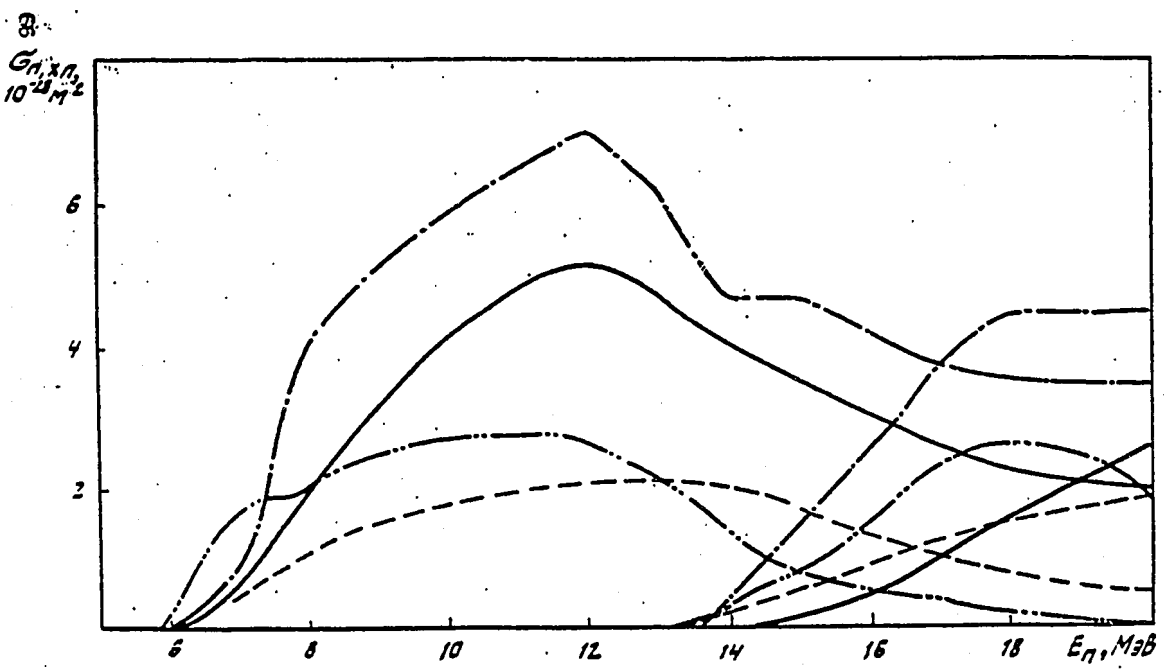

Fig. 4.7 Comparison of evaluated (n,2n) and (n,3n) reactions cross-sections : present evaluation _____ ;
Ref.100 JENDL-2 evaluation -..-..-..-
Ref.90 JENDL-3 evaluation - - - - - -
Ref.92 ENDL-78 evaluation -.-.-.-.-.

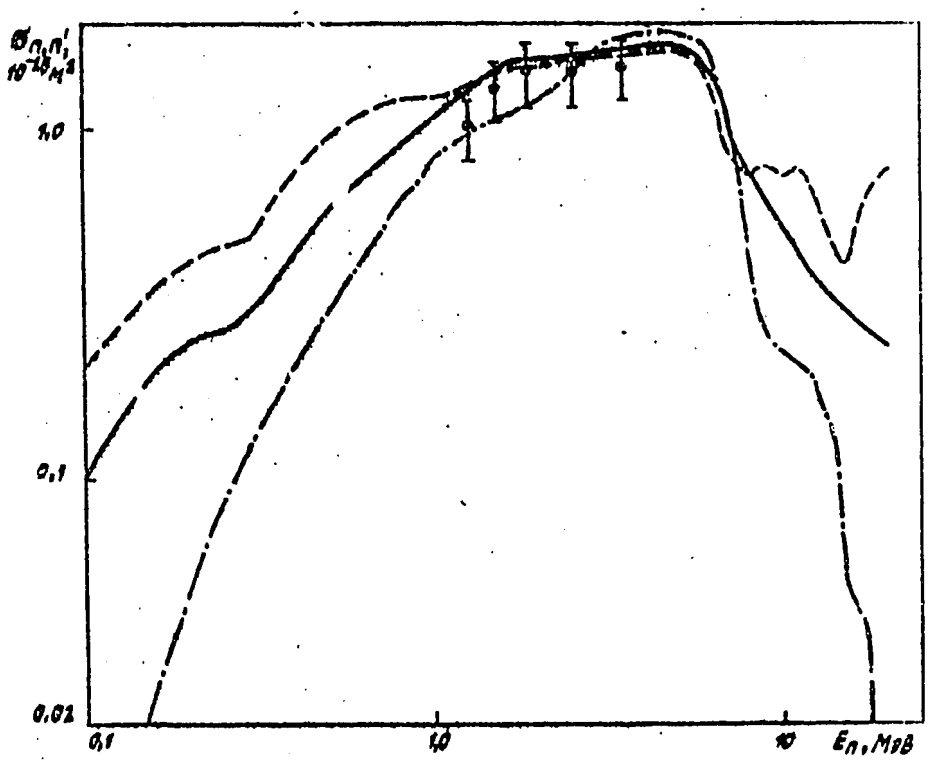

Fig. 4.8 Comparison of evaluated ^{233}U inelastic scattering ross-sections:
present evaluation _____ ;
Ref.90 JENDL-3 evaluation - - -
Ref.92 ENDL-78 evaluation
Ref.91 experimental data

Table 4.1

^{233}U levels scheme (Ref.77)

1	2	3	1	2	3	1	2	3
1	0.0	5/2+	12	353.7	9/2-	22	597.2	(7/2+)
2	40.35	7/2+	13	397.4	(11/2-)	23	646	-
3	92.0	9/2+	14	398.55	1/2+	24	748	(5/2-)
4	155.1	11/2+	15	415.78	3/2+	25	766	-
5	197	-	16	425	(17/2+)	26	790	(7/2-)
6	228	13/2+	17	503.5	7/2-	27	819	7/2-
7	298.85	(5/2-)	18	521	-	28	838	(9/2-)
8	311.95	3/2+	19	546.6	(5/2+)	29	865	-
9	318	(15/2+)	20	565	(9/2-)	30	898	-
10	320.7	(15/2+)	21	575	-	31	914	(11/2-)
11	340.5	5/2+	-	-	-	-	-	-

1. Level number
2. Level energy, keV
3. Level spin and parity

Table 4.2

Fission barrier parameters for U isotopes

Isotope	1	2	3	4
234	4.8	1.0	5.6	0.6
233	5.3	1.0	5.9	0.5
232	5.1	1.0	5.8	0.6

1 - E_f^A
2 - $\hbar\omega_A$
3 - E_f^B
4 - $\hbar\omega_B$

Table 4.3

Comparison of calculated scattering cross-sections and experimental data [91]

1	2	3	4	5
1.27	0.0-0.12	4.05 ± 0.162	3.89	3.69
1.49	0.0-0.13	4.01 ± 0.110	3.82	3.71
1.85	0.0-0.13	4.05 ± 0.118	3.94	3.90
2.55	0.0-0.20	4.57 ± 0.155	4.49	4.56
3.55	0.0-0.35	5.13 ± 0.170	4.96	5.04

1 - E_n (MeV)
2 - ΔE_x (MeV)
3 - $(\sigma_{exp} + \Delta\sigma_{exp})\, 10^{-28}$ m^2
4 - σ_{cal} 10^{-28} m^2
5 - JENDL-3

Table 4.4

Evaluated data from neutron cross-sections for ^{233}U in the fast neutron energy region, 10^{-28} m^2

E_n MeV	σ_t	σ_n	σ_f	σ_γ	$\sigma_{n'}$ Direct	$\sigma_{n'}$ Total	σ_{in}	σ_{an}
I	2	3	4	5	6	7	8	9
0,04	I3,400	I0,593	2,530	0,277				
0,05	I3,I50	I0,409	2,440	0,272	0,00I	0,029		
0,06	I2,887	I0,I98	2,374	0,268	0,003	0,047		
0,08	I2,449	9,825	2,29I	0,257	0,005	0,07I		
0,I0	I2,086	9,506	2,230	0,245	0,009	0,I05		
0,I2	II,756	9,I97	2,I86	0,233	0,0I5	0,I40		
0,I4	II,460	8,9I7	2,I44	0,222	0,022	0,I77		
0,I6	II,2I0	8,670	2,I23	0,2I2	0,029	0,205		
0,I8	I0,950	8,39I	2,I26	0,208	0,036	0,225		
0,20	I0,7I6	8,I36	2,I37	0,200	0,044	0,243		
0,22	I0,500	7,89I	2,I57	0,I97	0,053	0,255		
0,24	I0,285	7,652	2,I73	0,I96	0,06I	0,264		
0,26	I0,078	7,436	2,I73	0,I96	0,067	0,273		
0,28	9,882	7,243	2,I58	0,I94	0,073	0,287		
0,30	9,695	7,072	2,I25	0,I90	0,079	0,308		
0,32	9,5I6	6,890	2,II2	0,I85	0,084	0,329		
0,34	9,345	6,707	2,I05	0,I79	0,089	0,354		
0,36	9,I82	6,535	2,095	0,I72	0,094	0,380		
0,38	9,024	6,374	2,076	0,I66	0,099	0,408		
0,40	8.876	6,222	2,062	0,I60	0,I03	0,432		
0,42	8,732	6,079	2,038	0,I54	0,I07	0,46I		
0,44	8,596	5,944	2,0I3	0,I49	0,III	0,490		
0,46	8,466	5,8I5	I,988	0,I44	0,II5	0,5I9		
0,48	8,342	5,69I	I,960	0,I39	0,II9	0,552		
0,50	8,223	5,57I	I,938	0,I35	0,I24	0,579		
0,55	7,95I	5,2886	I,900	0,I23	0,I34	0,6394		
0,60	7,7I7	5,0224	I,893	0,II5	0,I45	0,6866		
0,65	7,529	4,7946	I,893	0,I07	0,I54	0,7344		
0,70	7,365	4,5980	I,885	0,098	0,I63	0,7840		
0,75	7,22I	4,4306	I,863	0,092	0,I72	0,8354		
0,80	7,I02	4,2877	I,843	0,085	0,I8I	0,8863		
0,85	7,000	4,I555	I,83I	0,080	0,I89	0,9335		
0,90	6,92I	4,0382	I,826	0,075	0,I97	0,98I8		
0,95	6,857	3,9359	I,826	0,07I	0,206	I,024I		
I,0	6,800	3,8439	I,826	0,066	0,2I4	I,064I		
I,I	6,7I8	3,6908	I,830	0,060	0,23I	I,I372		
I,2	6,689	3,5857	I,837	0,054	0,248	I,2I23		
I,3	6,689	3,5II6	I,855	0,048	0,264	I,2744		
I,4	6,720	3,4754	I,858	0,044	0,279	I,3426		
I,5	6,775	3,4665	I,860	0,040	0,294	I,4085		

Table 4.4 (continued)

I	2	3	4	5	6	7	8	9
I,6	6,85I	3,4826	I,874	0,037	0,307	I,4574		
I,8	7,022	3,566I	I,900	0,032	0,327	I,5239		
2,0	7,I95	3,69I4	I,926	0,027	0,339	I,5506		
2,2	7,368	3,843	I,9I0	0,024	0,346	I,59I		
2,4	7,559	4,03I	I,890	0,022	0,350	I,6I6		
2,6	7,660	4,I6I	I,868	0,0I9	0,348	I,6I2		
2,8	7,78I	4,3II	I,840	0,0I7	0,345	I,6I3		
3,0	7,876	4,433	I,804	0,0I5	0,342	I,624		
3,2	7,938	4,524	I,768	0,0I4	0,337	I,632		
3,4	7,983	4,593	I,736	0,0I3	0,333	I,64I		
3,6	8,006	4,638	I,7I2	0,0I2	0,328	I,644		
3,8	8,0I4	4,663	I,682	0,0II	0,323	I,658		
4,0	7,996	4,662	I,656	0,0I0	0,3I7	I,668		
4,2	7,957	4,64I	I,632	0,0095	0,3I2	I,6745		
4,4	7,906	4,605	I,607	0,0088	0,306	I,6852		
4,6	7,84I	4,555	I,584	0,0082	0,300	I,6938		
4,8	7,764	4,49I	I,560	0,0076	0,294	I,7054		
5,0	7,67I	4,4I2	I,538	0,0072	0,288	I,7I38		
5,5	7,4I2	4,I84	I,49I	0,0060	0,274	I,73I0		
6,0	7,I25	3,925	I,650	0,0052	0,262	I,5378	0,007	
6,5	6,856	3,677	I,924	0,0045	0,249	I,2245	0,026	
7,0	6,632	3,464	2,075	0,0040	0,237	I,0220	0,067	
7,5	6,43I	3,27I	2,I75	0,0035	0,225	0,8535	0,I28	
8,0	6,255	3,I03	2,2I0	0,003I	0,2I2	0,7479	0,I9I	
8,5	6,I03	2,96I	2,205	0,0027	0,202	0,6833	0,25I	
9,0	5,976	2,845	2,I85	0,0024	0,I9I	0,6296	0,3I4	
9,5	5,878	2,756	2,I75	0,0022	0,I82	0,5778	0,367	
I0,0	5,802	2,69I	2,I70	0,0020	0,I75	0,5270	0,4I2	
I0,5	5,750	2,652	2,I60	0,00I8	0,I7I	0,49I2	0,445	
II,0	5,720	2,634	2,I50	0,00I6	0,I69	0,4544	0,480	
II,5	5,709	2,636	2,I40	0,00I4	0,I66	0,4266	0,505	
I2,0	5,7I7	2,658	2,I50	0,00I2	0,I64	0,3958	0,5I4	
I2,5	5,739	2,690	2,I80	0,00I	0,I62	0,369	0,499	
I3,0	5,772	2,738	2,220	0,00I	0,I58	0,344	0,469	
I3,5	5,8II	2,790	2,250	0,00I	0,I56	0,332	0,437	0,00I
I4,0	5,855	2,853	2,265	0,00I	0,I52	0,320	0,4II	0,005
I4,5	5,899	2,9I8	2,275	0,00I	0,I48	0,3II	0,383	0,0II
I5,0	5,943	2,986	2,280	0,00I	0,I45	0,30I	0,356	0,020
I6,0	6,033	3,II7	2,275	0,00I	0,I40	0,282	0,302	0,056
I7,0	6,III	3,240	2,240	0,00I	0,I33	0,267	0,257	0,I06
I8,0	6,I75	3,346	2,I90	0,00I	0,I28	0,257	0,223	0,I58
I9,0	6,223	3,433	2,I35	0,00I	0,I2I	0,243	0,203	0,208
20,0	6,252	3,495	2,060	0,00I	0,II8	0,240	0,I96	0,260

Table 4.5

Evaluated level excitation cross-sections for ^{233}U, 10^{-28} m^2

E_n, MeV	Level excitation energy, E_q, keV							
	40,35	92,0	155,1	40,35	92,0	155,1	228,0	298,0
	Direct excitation			Compounds nucleus mechanism				
1	2	3	4	5	6	7	8	9
0,05	0,0010			0,028				
0,06	0,0030			0,044				
0,08	0,0050			0,071				
0,10	0,0090			0,093	0,003			
0,12	0,0140	0,0010		0,111	0,014			
0,14	0,0200	0,0020		0,129	0,026			
0,16	0,0255	0,0035		0,139	0,037			
0,18	0,0304	0,0056		0,142	0,044	0,003		
0,20	0,0355	0,0085		0,143	0,050	0,006		
0,22	0,0405	0,0123	0,0002	0,141	0,053	0,008		
0,24	0,0451	0,0156	0,0003	0,138	0,055	0,010		
0,26	0,0488	0,0178	0,0004	0,136	0,058	0,012		
0,28	0,0525	0,0200	0,0005	0,138	0,062	0,014		
0,30	0,0562	0,0221	0,0007	0,146	0,067	0,016		
0,32	0,0590	0,0241	0,0009	0,144	0,068	0,017	0,001	0,013
0,34	0,0618	0,0261	0,0011	0,141	0,068	0,018	0,001	0,019
0,36	0,0645	0,0281	0,0013	0,137	0,068	0,019	0,001	0,023
0,38	0,0675	0,0300	0,0015	0,134	0,068	0,020	0,001	0,027
0,40	0,0693	0,0319	0,0016	0,132	0,068	0,021	0,002	0,030
0,42	0,0712	0,0337	0,0021	0,132	0,069	0,022	0,002	0,033
0,44	0,0731	0,0355	0,0024	0,131	0,070	0,023	0,002	0,036
0,46	0,0749	0,0374	0,0027	0,131	0,071	0,024	0,003	0,038
0,48	0,0766	0,0393	0,0031	0,131	0,073	0,025	0,003	0,041
0,50	0,0792	0,0413	0,0035	0,130	0,074	0,026	0,003	0,043
0,55	0,0837	0,0457	0,0046	0,1279	0,074	0,0275	0,005	0,046
0,60	0,0891	0,0500	0,0059	0,1244	0,072	0,0292	0,006	0,047
0,65	0,0934	0,0534	0,0072	0,1216	0,0714	0,0304	0,008	0,048
0,70	0,0975	0,0569	0,0086	0,1179	0,0702	0,0319	0,009	0,048
0,75	0,1020	0,0600	0,0100	0,1138	0,0697	0,0329	0,010	0,047
0,80	0,1057	0,0639	0,0114	0,1103	0,0680	0,0340	0,012	0,046
0,85	0,1092	0,0669	0,0129	0,1065	0,0670	0,0350	0,014	0,045
0,90	0,1125	0,0701	0,0144	0,1028	0,0660	0,0360	0,015	0,043
0,95	0,1165	0,0736	0,0159	0,0985	0,0640	0,0366	0,016	0,041
1,0	0,1198	0,0768	0,0174	0,0941	0,0620	0,0370	0,017	0,039
1,1	0,1276	0,0830	0,0204	0,0852	0,0580	0,0370	0,018	0,035
1,2	0,1352	0,0892	0,0236	0,0763	0,0540	0,0350	0,018	0,031
1,3	0,1426	0,0947	0,0267	0,0674	0,0490	0,0330	0,018	0,027
1,4	0,1501	0,0998	0,0291	0,0584	0,0444	0,0308	0,017	0,023
1,5	0,1577	0,1053	0,0310	0,0495	0,0390	0,0280	0,016	0,020
1,6	0,1646	0,1098	0,0329	0,0414	0,0330	0,0240	0,015	0,017
1,8	0,1756	0,1157	0,0357	0,0279	0,0240	0,0180	0,011	0,013
2,0	0,1826	0,1196	0,0368	0,0186	0,0160	0,0120	0,007	0,008
2,2	0,1873	0,1216	0,0371	0,0120	0,0100	0,0080	0,005	0,006
2,4	0,1906	0,1225	0,0369	0,0070	0,0070	0,0050	0,003	0,004
2,6	0,1902	0,1220	0,0358	0,005	0,0040	0,0030	0,002	0,002
2,8	0,1895	0,1207	0,0348	0,003	0,003	0,002	0,001	0,002
3,0	0,1886	0,1196	0,0338	0,002	0,002	0,001	0,001	0,001
3,2	0,1866	0,1178	0,0326	0,001	0,001	0,001	0,001	0,001
3,4	0,1851	0,1163	0,0316	0,001	0,001			
3,6	0,1827	0,1146	0,0307	0,001	0,001			

Table 4.5 (continued)

E_n MeV	Level energy E_q, keV								
	3II,0	3I8,0	320,7	340,5	353,7	397,4	4I5,78	425,0	503,5
I	2	3	4	5	6	7	8	9	I0
0,32	0,002								
0,34	0,008		0,0I0						
0,36	0,0I4		0,0I5	0,007	0,002				
0,38	0,02I		0,0I8	0,0I5	0,005				
0,40	0,026		0,02I	0,022	0,007				
0,42	0,032		0,025	0,030	0,008	0,00I			
0,44	0,036		0,028	0,037	0,0I0	0,00I	0,005		
0,46	0,040		0,030	0,043	0,0I2	0,002	0,0I0		
0,48	0,046	0,00I	0,033	0,050	0,0I4	0,002	0,0I4		
0,50	0,049	0,00I	0,035	0,056	0,0I6	0,003	0,0I9		
0,55	0,055	0,00I	0,039	0,065	0,0I9	0,005	0,030		0,0I0
0,60	0,057	0,002	0,040	0,070	0,02I	0,006	0,036		0,0I5
0,65	0,058	0,002	0,04I	0,07I	0,022	0,007	0,040		0,0I9
0,70	0,058	0,002	0,04I	0,072	0,023	0,009	0,043		0,022
0,75	0,058	0,003	0,04I	0,072	0,024	0,0I0	0,045		0,025
0,80	0,057	0,004	0,04I	0,072	0,025	0,0II	0,046		0,027
0,85	0,055	0,004	0,040	0,070	0,025	0,0II	0,046		0,028
0,90	0,053	0,005	0,039	0,068	0,025	0,0I2	0,045		0,028
0,95	0,05I	0,005	0,037	0,065	0,025	0,0I2	0,044		0,028
I,0	0,049	0,006	0,036	0,062	0,025	0,0I3	0,042	0,00I	0,027
I,I	0,044	0,007	0,033	0,056	0,023	0,0I3	0,039	0,00I	0,025
I,2	0,040	0,007	0,030	0,050	0,022	0,0I3	0,035	0,00I	0,024
I,3	0,036	0,007	0,026	0,044	0,020	0,0I2	0,032	0,002	0,02I
I,4	0,032	0,007	0,023	0,039	0,0I8	0,0II	0,029	0,002	0,0I9
I,5	0,028	0,007	0,020	0,035	0,0I6	0,0I0	0,026	0,002	0,0I7
I,6	0,024	0,007	0,0I7	0,03I	0,0I4	0,009	0,023	0,002	0,0I5
I,8	0,0I8	0,005	0,0I3	0,023	0,0I0	0,007	0,0I7	0,002	0,0II
2,0	0,0I2	0,004	0,008	0,0I5	0,007	0,005	0,0I2	0,002	0,008
2,2	0,008	0,003	0,006	0,0I0	0,005	0,003	0,008	0,00I	0,005
2,4	0,006	0,002	0,004	0,007	0,003	0,002	0,005	0,00I	0,004
2,6	0,003	0,00I	0,002	0,004	0,002	0,002	0,003	0,00I	0,002
2,8	0,002	0,00I	0,002	0,003	0,00I	0,00I	0,002		0,002
3,0	0,00I		0,00I	0,002	0,00I	0,00I	0,00I		0,00I
3,2	0,00I		0,00I	0,00I	0,00I		0,00I		0,00I
3,4				0,00I					

Table 4.5 (continued)

E_n MeV	Level energy, E_q, keV			Continuous spectrum excitation 10^{-28} m²
	40,35	92,0	I55,I	
	Direct excitation, 10^{-28} m²			
3,8	0,I806	0,II27	0,0297	I,335
4,0	0,I775	0,II08	0,0287	I,35I
4,2	0,I75	0,I09	0,028	I,3625
4,4	0,I72	0,I07	0,027	I,3792
4,6	0,I69	0,I05	0,026	I,3938
4,8	0,I66	0,I03	0,025	I,4II4
5,0	0,I63	0,I0I	0,024	I,4258
5,5	0,I56	0,096	0,022	I,4570
6,0	0,I50	0,092	0,020	I,2758
6,5	0,I44	0,087	0,0I8	0,9755
7,0	0,I38	0,083	0,0I6	0,7850
7,5	0,I32	0,079	0,0I4	0,6285
8,0	0,I26	0,074	0,0I2	0,5359
8,5	0,I2I	0,070	0,0II	0,48I3
9,0	0,II5	0,066	0,0I0	0,4386
9,5	0,II0	0,063	0,009	0,3958
I0,0	0,I06	0,060	0,009	0,3520
I0,5	0,I04	0,059	0,008	0,3202
II,0	0,I03	0,058	0,008	0,2854
II,5	0,I02	0,057	0,007	0,2606
I2,0	0,I0I	0,056	0,007	0,23I8
I2,5	0,I00	0,055	0,007	0,207
I3,0	0,098	0,054	0,006	0,I86
I3,5	0,097	0,053	0,006	0,176
I4,0	0,095	0,05I	0,006	0,I68
I4,5	0,093	0,050	0,005	0,I63
I5,0	0,09I	0,049	0,005	0,I56
I6,0	0,088	0,047	0,005	0,I42
I7,0	0,085	0,044	0,004	0,I34
I8,0	0,082	0,042	0,004	0,I29
I9,0	0,078	0,040	0,003	0,I22
20,0	0,076	0,039	0,003	0,I22

Table 4.5 (continued)

E_n MeV	Level energy, E_q, keV			Continuous spectrum excitation 10^{-28} m²
	546,6	565,0	597,0	
0,55	0,00I			
0,60	0,0I2	0,004		
0,65	0,02I	0,006	0,009	0,005
0,70	0,030	0,009	0,0I7	0,0I8
0,75	0,037	0,0II	0,024	0,040
0,80	0,042	0,0I3	0,030	0,067
0,85	0,045	0,0I5	0,034	0,I04
0,90	0,046	0,0I6	0,037	0,I48
0,95	0,046	0,0I7	0,038	0,I94
I,0	0,046	0,0I7	0,039	0,238
I,I	0,043	0,0I7	0,038	0,334
I,2	0,039	0,0I6	0,036	0,437
I,3	0,036	0,0I5	0,033	0,532
I,4	0,033	0,0I4	0,030	0,633
I,5	0,029	0,0I3	0,027	0,732
I,6	0,025	0,0II	0,024	0,8I8
I,8	0,020	0,009	0,0I9	0,949
2,0	0,0I4	0,006	0,0I3	I,044
2,2	0,009	0,004	0,009	I,I33
2,4	0,006	0,003	0,006	I,I92
2,6	0,004	0,002	0,004	I,2I8
2,8	0,002	0,00I	0,003	I,237
3,0	0,002	0,00I	0,002	I,262
3,2	0,00I	0,00I	0,00I	I,28I
3,4	0,00I		0,00I	I,303
3,6			0,00I	I,3I3

5. EVALUATION OF SECONDARY NEUTRON CHARACTERISTICS AND OF ν FOR ^{233}U

The experimental information on secondary neutron energy and angular distributions for ^{233}U is insufficient for evaluations to be based on it alone. We therefore used theoretical calculations and systematics with parameters tested against available experimental data.

5.1. Evaluation of secondary neutron energy spectra

There have been no measurements of secondary neutron energy spectra for any reaction except fission. Thus, the evaluated spectra of neutrons emitted in the reaction (n,n') and of neutrons successively emitted in the reactions (n,2n) and (n,3n) have been calculated using a statistical model with allowance for possible pre-equilibrium emission of the first neutron, for fission competition and for other processes occurring in the successive stages of decay [103].

The spectra or the average energies of prompt fission neutrons have been measured in a number of studies [104, 105], but only at low incident neutron energies, which means that the energy dependence of the temperature or average spectrum energy cannot be determined. In most works experimental data have been represented by Maxwellian-type distributions:

$$N_M(E) = \frac{2}{\sqrt{\pi}\cdot T_M^{3/2}}\cdot\sqrt{E}\cdot \exp(-E/T_M)$$

where T_M = 1.32-1.34.

There are experimental indications of and theoretical arguments for [106] a deviation of the form of prompt fission neutron spectra from a Maxwellian distribution. However, such deviations are substantial only at secondary neutron energies > 8-10 MeV, which never account for more than ~ 1% of the spectrum. In view of this and given the accuracy which has been achieved in measuring prompt fission neutron spectra for ^{233}U, in the work described here we used the Maxwellian form of the dependence to describe the evaluated prompt fission neutron spectra. The spectrum temperature was evaluated on the basis of

available experimental data for an incident thermal neutron energy T_M = 1.325 MeV. The energy dependence $T_M(E_n)$ is given in the form predicted by systematics [107]:

$$T_M(E) = a + b\,[1+\bar{\nu}(E)]^{1/2}$$

where

$$\bar{\nu}(E) = \nu_t(E) - \frac{\sigma_{nn'f}(E)}{\sigma_{nF}(E)} - 2\cdot\frac{\sigma_{n2nf}(E)}{\sigma_{nF}(E)}.$$

The chosen coefficients a = 0.611 and b = 0.382 were such that they matched the value of T_M at thermal and ensured an increase of approximately 1% in that value as the incident neutron energy increased to 1 MeV. The evaluated fission spectrum temperature values are given in Table 5.1.

Table 5.1

Temperature of Fission Neutron Spectra, Mev

E_n, MeV	T_M	E_n, MeV	T_M	E_n, MeV	T_M
10-5	1.325	4.5	1.380	13	1.428
1.0	1.333	6.5	1.384	15	1.431
2.2	1.347	9.5	1.407	20	1.461

5.2. $\bar{\nu}_t$ for ^{233}U

Detailed analyses of the experimental data obtained in measurements of the average number of prompt fission neutrons $\bar{\nu}_t$ for ^{233}U have been conducted [108, 109]. After the publication of a review by V.V. Malinovskij et al. [109], R. Gwin et al. published a paper [110] in which $\bar{\nu}_p(^{233}U)/\bar{\nu}^{sp}_p(^{252}Cf)$ was measured for energies up to 10 MeV.

In evaluating $\bar{\nu}_p(E)$ we used only experimental data obtained by measuring $\nu_p(^{233}U)$ relative to the average number of prompt neutrons from the spontaneous fission of ^{252}Cf and all available information for the 14-15 MeV energy region. All the data were renormalized to $\bar{\nu}^{sp}_p(^{252}Cf)$ = 3.757 and $\nu^{th}_p(^{233}U)$ = 2.485 and fitted using the least squares method.

The evaluated dependence $\bar{\nu}_p(E)$ is presented in the form

$$\bar{\nu}_p(E_n) = \begin{cases} 2{,}485 - 0{,}061 \cdot E_n + 0{,}244 \cdot E_n^2 - 0{,}1\, E_n^3, & 10^{-8} \leq E_n \leq 1 \text{ МэВ}; \\ 2{,}452 + 0{,}116 \cdot E_n, & 1 \leq E_n \leq 2{,}2 \text{ МэВ}; \\ 2{,}386 + 0{,}146 \cdot E_n, & 2{,}2 \leq E_n \leq 9{,}625 \text{ МэВ}; \\ 2{,}848 + 0{,}098 \cdot E_n, & 9{,}625 \leq E_n \leq 20 \text{ МэВ}. \end{cases}$$

A review of experimental data and an evaluation of the energy dependence of the average number of secondary neutrons for ^{233}U have also been carried out [108]. In the light of subsequently published experimental data [111], it became necessary to slightly increase the evaluated $\bar{\nu}_d(^{233}U)$ in the energy region up to 4.5 MeV.

The evaluated dependence $\nu_d(E_n)$ may be presented in the following form:

$$\nu_d(E_n) = \begin{cases} 0{,}0075, & 10^{-5} \leq E_n \leq 4{,}5 \text{ МэВ} \\ 0{,}0138 - 0{,}0014 \cdot E_n, & 4{,}5 \leq E_n \leq 6{,}5 \text{ МэВ} \\ 0{,}0047, & 6{,}5 \leq E_n \leq 13 \text{ МэВ} \\ 0{,}00795 - 0{,}00025 \cdot E_n, & 13 \leq E_n \leq 15 \text{ МэВ} \\ 0{,}0042, & 15 \leq E_n \leq 20 \text{ МэВ} \end{cases}$$

5.3. Angular distributions of scattered neutrons

The angular distributions of scattered neutrons have been measured only at two energy points 0.7 MeV and 1.5 MeV [89] for elastic and inelastic scattering at the first two levels. As the coupled-channels method gives a good description of the angular distributions of scattered neutrons, it was used for obtaining evaluated distributions for scattering that is elastic and inelastic at the first three levels. The evaluated distributions include the isotropic part of these processes, which flow through the compound nucleus. The angular distributions of the neutrons scattered at the remaining levels and emitted in other reactions were assumed to be isotropic.

CONCLUSION

On the basis of an analysis of experiments and the results of theoretical calculations, ^{233}U neutron data were evaluated for incident neutron energies of 10^5 eV-20 MeV. The file of evaluated neutron constants for ^{233}U was transmitted to the

Nuclear Data Centre for inclusion in the BROND national library. The file contains data on neutron cross-sections, $\bar{\nu}$ and angular distributions and energy spectra of secondary neutrons. Cross-sections in the thermal (10^{-5}-1 eV) and resonance energy regions were evaluated on the basis of experimental data. The file includes resolved resonance parameters in the 1-100 eV energy region and unresolved parameters in the 0.1-40 keV region. In the fast neutron energy range, only the total cross-section and fission cross-section were evaluated on the basis of experimental data. In order to evaluate all other cross-sections we used theoretical calculations based on generalized optical and statistical models. Comparison showed that there is good agreement between the evaluated and the experimental data.

REFERENCES

[1] MUROGOV, V.M., TROYANOV, M.F. and SHMELEV, A.N., Use of Thorium in Nuclear Reactors, Ehnergoatomizdat, Moscow (1983) 96 pp [in Russian].

[2] MUROGOV, V.M., ZININ, A.I., ILYUNIN, V.G. and RUDNEVA, V. Ya., Fast Reactors with Different Types of Fuel in the Uranium-Plutonium and Mixed Fuel Cycles, Preprint FEhI-1920, Obninsk (1988) [in Russian].

[3] LORENZ, A., Proposed recommended List of heavy element radionuclide decay data, Report INDC(NDS)-149/NE, IAEA, Vienna (1983).

[4] HOWERTON, R.J., Threshold of nuclear reactions induced by neutrons, photons, protons, deuterons and alpha particles, Report UCRL-50400, TID-4500, UC-34, Vol.9, Livermore (1970).

[5] KRAVTSOV, V.A., Atomic Masses and the Binding Energies of Nuclei, Atomizdat, Moscow (1974) 344 pp [in Russian].

[6] KOLAR, W., CARRARO, G., NASTRI, G., "Total neutron cross-section of ^{233}U from 0.7 to 320 eV" in Proc. Inter. Conf. on Nuclear Data for Reactors, Vol.2, Helsinki (1970) 387-402.

[7] BROOKS, F.D., JOLY, J.E., SCHOMBERG, M.Q., SOWERBY, M.G., Eta and neutron cross-sections of ^{239}Pu and ^{233}U, Report AERE-M-1709 (1966).

[8] VERTEBNYJ, V.P., VLASOV, M.F., KOLOTYJ, V.V., et al., Total neutron cross-sections of ^{233}U and ^{235}U and the slow neutron scattering cross-section for ^{233}U, in: Nuclear Physics Research in the USSR, 16 (1973) 8-10 [in Russian].

[9] PSHENICHNYJ, V.A., BLANKOVSKIJ, A.I., GNIDAK, N.L. and PAVLENKO, E.A., Measurement of the ^{233}U energy dependence in the 0.02-1 eV energy region, in: Nuclear Physics Research in the USSR, 21 (1976) 29-37 [in Russian].

[10] SAILOR, V.L., Neutron resonances in ^{233}U and ^{235}U, Phys.Rev. 100 (1955) 1249.
[11] MOORE, M.S., MILLER, L.G., SIMPSON, O.D., Slow neutron total and fission cross-sections of ^{233}U, Phys.Rev. 118 (1960) 714.
[12] HARVEY, J.A., MOORE, C.L., HILL, N.W., "Neutron total cross-sections of ^{233}U from 0.01 to 1.0 eV", in Proc. Intern. Conf. on Nuclear Cross-sections and Technology, Knoxville (1979) 690.
[13] BLOCK, R.C., SLAUGHTER, G.G., HARVEY, G.A., Thermal neutron cross-section measurements of ^{233}U, ^{235}U, ^{240}Pu, ^{234}U and ^{129}I with the ORNL fast chopper time-of-flight neutron spectrometer, Nucl. Sci. Eng. 8 (1960) 112.
[14] MUETHER, H.R., PALEVSKY, H., Priv. Comm., Brookhaven National Laboratory (1955).
[15] PATTENDEN, N.J., HARVEY, J.A., Measurement of the neutron total cross-section of ^{233}U, Nucl. Sci. Eng. 17 (1963) 404.
[16] CAO, M.G., MIGNECO, E., THEOBALD, J.P., MERLA, M., Proc. Intern. Conf. on Nuclear Data for Reactors, Vol.1, Helsinki (1970) 419.
[17] DERYUTTER, A.J., WAGEMANS, C., Measurement and normalization of the relative ^{233}U fission cross-section in the low resonance region, Nucl. Sci. Eng. 54 (1974) 423.
[18] SANDERS, J.E., PRICE, B.T., RICHMOND, R., Fission cross-sections as a function of neutron energy III, uranium-133, Report NRDC-81 (1955).
[19] WESTON, L.W., GWIN, R., De SAUSSURE, G., et al., Neutron fission and capture cross-section measurements for ^{233}U in the energy region 0.02 to 1 eV, Nucl. Sci. Eng. 42 (1970) 143.
[20] WESTON, L.W., GWIN, R., De SAUSSURE, G., et al., Measurement of the neutron fission and capture cross-sections for ^{233}U in the energy region 0.4 to 2000 eV, Nucl. Sci. Eng. 34 (1968) 1-7.
[21] OLECSA, S. Neutron scattering cross-sections of ^{233}U, Phys. Rev. 109 (1958) 1645.
[22] SANDERS, J.E., SCARSGAARD H.M., KENWARD, C.J., The energy dependence of the fission neutron yield per neutron absorbed in ^{233}U over the range 0.125 - 2.2 eV, Nucl. Energy 5 (1957) 186-191.
[23] SMITH, J.R., REEDER, S.D., "Measurement of the absolute value of eta for ^{241}Pu by the manganese bath method", Proc. Intern. Conf. on Neutron Cross-sections and Technology, Vol.1, Washington, (1968) 589-596.
[24] SMITH, J.R., REEDER, S.D., Low energy eta measurements, Report IN-1407 (1970).
[25] MAGLEBY, E.H., SMITH, J.R., EVANS, J.E., MOORE, M.S., "Energy dependence of eta for uranium-233 in the region 0.11 to 4.0 eV", in Proc. Intern Conf. on Neutron Cross-Sections and Technology, Washington (1966) 919.

[26] PALEVSKY, H., HUGHES, D.J., ZIMMERMAN, R.L., EISBERG, R.M., Direct measurement of the energy variation of eta for ^{233}U, ^{235}U and ^{239}Pu, J. of Nucl. Energy 3 (1956) 177-187.
[27] DIVADEENAM, M., STEHN, J.R., "A least squares fit of thermal data for fissile nuclei", Nuclear Standards Reference Data, TECDOC-335, Vienna (1985) 238-241.
[28] ANTSIPOV, G.V., KON'SHIN, V.A. and MOROGOVSKIJ, G.B., FORTRAN programs for the approximation of experimental data using orthogonal polynomials with statistical analysis, Problems of Atomic Science and Technology, ser. Nuclear constants, 10 (1972) 262-271 [in Russian].
[29] DRAKE, M.K., DAHLBERG, R.C., McGEHEE, B.G., Neutron cross-sections for uranium-233, Report GA-7076, General Atomics(1966).
[30] MOORE, M.S., MOSES, J.D., KEYWORTH, G.A., et al., Spin determination of resonance structure in ^{235}U+n below 25 KeV, Phys. Rev. C. 18 (1978) 1328-1348.
[31] NIZAMUDDIN, S., BLONS, J., Single level analysis of the uranium-233 fission cross-section for neutron energies between 6 and 124 eV, Nucl. Sci. Eng. 54 (1974) 116-126.
[32] BLONS, J., High resolution measurements of neutron-induced fission cross-sections for ^{233}U, ^{235}U, ^{239}Pu and ^{241}Pu below 30 keV, Nucl. Sci. Eng. 51 (1973) 130-147.
[33] MOROGOVSKIJ, G.B., Re-evaluation of ^{241}Pu resonance parameters, in: Problems of Atomic Science and Technology, ser. Nuclear constants, No. 3 (1988) 17-20 [in Russian].
[34] MUGHABGHAB, S.F., Neutron Cross-sections, Report BNL-325, Vol.1, Orlando, Florida (1984).
[35] MOROGOVSKIJ, G.B., ^{235}U resonance parameters in the 1-100 eV energy range, in: Problems of Atomic Science and Technology, ser. Nuclear constants, No. 1 (1986) 12-20 [in Russian].
[36] FULWOOD, R., MORGAN, E., YEATER, M., Prog. Report KAPL-1770, New York (1957).
[37] POENITZ, W.P., WHALEN, J.F., GUENTER, P., SMITH, A.B., Measurement of the total neutron cross-section of ^{233}U between 40 keV and 4.5 MeV, Nucl. Sci. Eng. 68 (1978) 358.
[38] BLONS, J., DERRIEN, H., MICHAUDON, A., "Measurement and analysis of the fission cross-section of ^{233}U for neutron energies below 30 keV", in Proc. Conf. on Nuclear Cross-Sections and Technology, Vol.1, Knoxville 1971, Washington (1975) 829-835.
[39] GWIN, R., SILVER, E., INGLE, R.W., WEAVER, H., Measurement of the neutron capture and fission cross-sections of ^{239}Pu and ^{235}U, Nucl. Sci. Eng. 59 (1976) 79-105.
[40] MOSTOVAYA, T.A., MOSTOVOJ, V.I., BIRYUKOV, S.A., et al., Measurements of ^{233}U and ^{235}U fission cross-sections in the 0.1-100 keV energy region and $^{233}U/^{235}U$ fission cross-section ratios up to 2 MeV, in: Neutron Physics (Proc. 5th All-Union Neutron Physics Conference, Kiev, 1980) TsNIIatominform, Moscow (1980) Part 3, 30-34 [in Russian].

[41] BERGMAN, A.A., KOLOSOVSKIJ, A.G. MEDVEDEV, A.N., et al., Measurement of the ^{233}U fission cross-section and its relation to the ^{235}U fission cross-section in the 100 eV to 50 keV neutron energy region, Neutron Physics (Proc. 5th All-Union Neutron Physics Conference, Kiev, 1980) TsNIIatominform, Moscow (1980) Part 3, 54-57 [in Russian].
[42] BERGEN, D., Fission cross-sections from Pommard, Report LA-4420, Los Alamos (1970).
[43] ALBERT, R.D., ^{233}U fission cross-section measured using a nuclear explosion in space, Phys. Rev. 142 (1966) 778-787.
[44] BOHR, O. and MOTTELSON, B., Structure of the Atomic Nucleus [translation into Russian] Mir, Moscow (1977) 2, 664 pp.
[45] IGNATYUK A.V., ISTEPOV, K.K. and SMIRENKIN, G.N., The role of collective effects in level density systematics, Nuclear Physics, 29 (1979) 875-883 [in Russian].
[46] LYNN, J.E., Systematics for neutron reactions of the actinide nuclei, Report AERE-R-7468, Harwell (1974).
[47] PORODZINSKIJ, Yu.V. and SUKHOVITSKIJ, E.Sh., Method for determining average neutron widths and average distances between levels taking into account the finite resolution of the experimental instrumentation, Proc. Acad. Sciences of Byelorussian SSR, ser. Physics and energy, No. 3 (1986) 19-23 [in Russian].
[48] KIKUCHI, Y., Evaluation of neutron nuclear data for ^{233}U in the thermal and resonance regions, Report JAERI-M-9318, Tokyo (1981).
[50] DUSHIN, V.N., FOMICHEV, A.V., KOVALENKO, S.S., et al., Statistical analysis of experimental data on ^{233}U, ^{235}U, ^{238}U, ^{237}Np, ^{239}Pu and ^{242}Pu fission cross-sections for neutrons with energies of 2.6, 8.5 and 14.5 MeV, Atomnaya Ehnergiya, 55 (1983) 218-222.
[51] ZASADNY, K.R., AGRAWAL, H.M., MAHDAVI, M., Measurement of the 14 MeV fission cross-sections for ^{233}U and ^{237}Np, Trans. Amer. Nucl. Soc. 47 (1984) 425-427.
[52] KALININ, V.A., KOVALENKO, S.S., KUZ'MIN, V.N., et al., Absolute measurements of ^{237}Np and ^{233}U fission cross-sections for neutrons with an energy of 1.9 MeV using the method of time-correlated coincident particles with magnetic analysis, Problems of Atomic Science and Technology, ser. Nuclear constants, No. 4 (1987) 3-10 [in Russian].
[53] POENITZ, W.P., Absolute measurement of the $^{233}U(n.f)$ cross-sections between 0.13 and 8.0 MeV, Report ANL/NDM-36, Argonne (1979).
[54] IYER, W., Report BARC, Bombay (1978).
[55] MEADOWS, J.W., The ratio of the uranium-233 to uranium-235 fission cross-section, Nucl. Sci. Eng. 54 (1974) 317-321.
[56] MEADOWS, J.W., The fission cross-sections of ^{230}Th, ^{232}Th, ^{233}U, ^{234}U, ^{236}U, ^{238}U, ^{239}Pu and ^{242}Pu relative to ^{235}U, Annals Nucl. Energy 15 (1988) 421-429.

[57] FURSOV, B.I., KUPRIYANOV, V.M. and SMIRENKIN, G.N., Measurement of ^{233}U and ^{241}Pu fission cross-sections relative to the ^{235}U fission cross-section in the 0.024-7.4 MeV neutron energy range, Atomnaya Ehnergiya 44 (1978) 236-239.
[58] KANDA, K., IMARUOKA, H., YOSHIDA, K., Measurement of fast neutron induced fission cross-sections of ^{232}Th, ^{233}U and ^{234}U relative to ^{235}U, in Conf.Proc. Nuclear Data for Basic and Applied Science, Santa-Fe (USA) (1985) 569.
[59] SHPAK, D.L. and KOROLEV, G.G., Measurement of ^{233}U and ^{235}U fission cross-section ratios in the 0.06-3.28 MeV neutron energy range, in Neutron Physics (Proc. 5th All-Union Neutron Physics Conference, Kiev, 1980) TsNIIatominform, Moscow (1980) Part 3, 35-39 [in Russian].
[60] WHITE, P.H., HODGKINSON, J.G., WALL, G.J., Measurement of the fission cross-section for neutrons of energies in the range 40-500 keV, in Conf. Proc. Physics and Chemistry of Fission, Vienna 1965,IAEA (1965) 219-233.
[61] WHITE, P.H., WARNER, G.P., The fission cross-sections of ^{233U}, ^{234}U, ^{236}U, ^{238}U, ^{237}Np, ^{239}Pu and ^{241}Pu relative to that of ^{235}U for neutrons in the energy range 1-14 MeV, J. Nucl. Energy 21 (1967) 671-679.
[62] NESTEROV, V.G. and SMIRENKIN, G.N., ^{233}U, ^{235}U and ^{239}Pu fission cross-section ratios for fast neutrons, in: Atomnaya ehnergiya 24 (1968) 185-187.
[63] PFLETCHINGER, R., KAPPELER, F., A measurement of the fission cross-sections of ^{239}Pu and ^{233}U relative to ^{235}U, Nucl. Sci. Eng. 40 (1970) 375-382.
[64 ALLEN, W.D., FERGUSON, A,T.G., "The fission cross-sections of ^{233}U, ^{235}U, ^{239}U and ^{239}Pu for neutrons in the energy range 0.030 to 30 MeV", Proc. Phys. Soc. Section A, 70 (1957) 573.
[65] SMITH, R.K., HENKEL, R.L., NOBLES, R.A., Neutron induced fission cross-sections for ^{233}U, ^{235}U, ^{238}U and ^{241}Pu from 2 to 10 MeV, Bull. Amer. Phys. Soc. Ser.II, 2 (1957) 196.
[66] ZHURAVLEV, K.D., KROSHKIN, N.I. and KARIN. L.V., ^{233}U fission cross-sections for neutrons with energies of 2, 24, 55 and 144 keV, in Neutron Physics (Proc. 4th All-Union Neutron Physics Conference, Kiev, 1977) TsNIIatominform, Moscow (1977) Part 3, 131-133 [in Russian].
[67] ZHURAVLEV, K.D., KROSHKIN, N.K. and KARIN, L.V., ^{235}U and ^{239}Pu fission cross-sections for neutrons with energies of 2, 24, 55 and 144 keV, Atomnaya ehnergiya 42 (1977) 56-57.
[68] ZHAGROV, E.A., NEMILOV, Yu. A., PLATONOV, A.V., et al., ^{233}U and ^{235}U fission cross-sections for intermediate neutron energies, in Neutron Physics (Proc. 5th All-Union Neutron Physics Conference, Kiev, 1980) TsNIIatominform, Moscow (1980) Part 3, 45-48 [in Russian].
[69] CARLSON, A.D., POENITZ, W.P., HALE, G.M., et al.,"The neutron cross-section standard evaluation for ENDF/B-VI", in Proc. Intern. Conf. on Nuclear Data for Science and Technology, Santa Fe (USA), Vol. 2 (1985) 1429.

[70] CARLSON, A.D., "NBS measurements of the ^{235}U fission cross-section", (Proc.IAEA Consultants Meeting on the ^{235}U Fast Neutron Fission Cross-Sections and the ^{252}Cf Fission Neutron Spectrum, Smolenice, 1983), Vienna (1983)61-67.
[71] STUPEGIA, D.C., Neutron total cross-section of ^{232}U, J. Nucl. Energy Parts A/B, 61 (1962) 201-203.
[72] FOSTER, D.J., GLASGOW, D.W., Neutron total cross-sections, 2.5 to 15 Mev, I.Experimental., Phys. Rev. C 3 (1971) 576.
[73] GREEN, L., MITCHELL, J.A., Total cross-section measurements with a ^{252}Cf time-of-flight spectrometer, Report WAPD-TM-1073 (1973).
[74] POENITZ, W.P., WHALEN, J.F., SMITH, A.B., Total neutron cross-sections of heavy nuclei, Nucl. Sci. Eng. 78 (1981) 333-341.
[75] POENITZ, W.P., WHALEN, J.F., Neutron total cross-section measurements in the energy range from 47 keV to 20 MeV, Report ANL-NDM-80 (1983)
[76] KLEPATSKIJ, A.B., KON'SHIN. V.A. and SUKHOVITSKIJ. E.Sh., The coupled-channel method and the evaluation of neutron data of fissile nuclei, Proc. Acad. Sciences of Byelorussian SSR, ser. Physics and energy, No. 2 (1984) 21-29 [in Russian].
[77] LEDERER, C.M., SHIRLEY, V.S., Table of Isotopes, 7th Ed., J. Wiley and Sons, New York (1978).
[78] IGNATYUK. A.V., KLEPATSKIJ, A.B., MASLOV, V.M., et al., Analysis of U and Pu isotope fission cross-sections for neutrons in the first "plateau" region, Nucl. Phys., 42 (1985) 569-577 [in Russian].
[79] MEYERS, W.D., SWIATECKI, W.S., Anomalies in nuclear masses, Ark. Physik 36 (1967) 343-353.
[80] AUCHAMPAUGH, G.F., BOWMAN, C.D., EVANS, J.E., Neutron induced fission cross-section of ^{232}U, Nucl. Phys. A112 (1968) 329-336.
[81] KUPRIYANOV, V.M., SMIRENKIN, G.N. and FURSOV, B.I., Systematics of neutron cross-sections and other characteristics of the probability of the fission of transuranic nuclei, Nucl. Phys. 39 (1984) 281-294 [in Russian].
[82] AXEL, P., Electric dipole ground-state transition width strength function and 7 MeV photon interactions, Phys. Rev. 126 (1962) 671-683.
[83] ZHUCHKO, V.E., OSTAPENKO, Yu. B., SMIRENKIN, G.K., et al., Investigation of the probability of the near-threshold fission of Th, U, Np, Pu and Am isotopes by γ-Bremsstrahlung, Nucl. Phys. 28 (1978) 1170-1183 [in Russian].
[84] SUKHOVITSKIJ, E.Sh., KLEPATSKIJ, A.B., KON'SHIN, V.A., et al., Allowance for the (n,γ) process in calculating the radiative capture widths and average cross-sections of fissioning nuclei, in Neutron Physics (Proc. 4th All-Union

Neutron Physics Conference, Kiev, 1977) TsNIIatominform, Moscow (1977) Part 4, 68-74 [in Russian].
[85] BJORNHOLM, S., STRUTINSKY, V.M., Intermediate states in fission, Nucl. Phys. A136 (1969) 1-24.
[86] HOWARD, W.M., MOLLER, P., Calculated fission barriers, ground state masses and particle separation energies for nuclei with $76 \leq Z \leq 100$ and $140 \leq N \leq 184$, Atom. Data and Nucl. Data Tables 25 (1980) 219-285.
[87] BACK, B.B., HANSEN, O., BRITT, H.C., et al., Fission of doubly even actinide nuclei induced by direct reactions, Phys. Rev. 9 (1974) 1924-1947.
[88] IGNATYUK, A.V. and MASLOV, V.M., Description of cross-sections for the fission of transuranic nuclei by fast neutrons, Nucl. Phys. 51 (1990) 1227-1237 [in Russian].
[89] HAOUOT, G., LACHKAR, Ch., LAGRANGE, Ch., et al., Neutron scattering cross-sections for ^{232}Th, ^{233}U, ^{235}U, ^{238}U, ^{239}Pu and ^{238}Pu between 0.6 and 3.4 MeV, Nucl. Sci. Eng. 81 (1982) 491-511.
[90] JAPANESE EVALUATED NUCLEAR DATA LIBRARY, Version 3, JAERI-1319, NEANDC(J)-150/U, INDC(JPN)-137/L (1990).
[91] SMITH, A.B., GUENTER, P.T., "On neutron inelastic scattering cross-sections of ^{232}Th, ^{233}U, ^{235}U, ^{238}U, ^{239}Pu and ^{240}Pu", in Proc. Intern. Conf. on Nuclear Data for Science and Technology, Antwerp (1982) 39.
[92] EVALUATED NUCLEAR DATA LIBRARY, ENDL-78, LLL, Report IAEA-NDC-11, Vienna (1979).
[93] HOPKINS, J.C., DIVEN, B.C., Neutron capture to fission ratios in ^{232}U, ^{235}U, ^{239}Pu, Nucl. Sci. Eng. 12 (1962) 169.
[94] SPIVAK, P.E., EROZOLIMSKIJ, B.G., DOROFEEV, G.A., et al., Average number of neutrons υ_{ef} emitted by ^{233}U, ^{235}U and ^{239}Pu isotopes during neutron capture at energies of 30-900 keV, Atomnaya Ehnergiya, 1 (1956) 21.
[95] KONONOV, V.N. and POLETAEV, E.D., Status of experimental data on alpha ^{239}Pu, Atomnaya Ehnergiya, 45 (1978) 187-192.
[96] BELANOVA, T.S., IGNATYUK, A.V., PASHCHENKO, A.B., et al., Radiative Neutron Capture, Ehnergoatomizdat, Moscow (1986) 248 pp [in Russian].
[97] FURSOV, B.I., BARANOV, E.Yu., KLEMYSHEV, M.P., et al., Measurement of the cross-section for ^{232}U fission in the 0.06-7.4 MeV neutron energy range, Atom. Ehnerg. 61 (1986)
[98] BRITT, H.C.,WILHELMI, J.B., Simulated (n,f) cross-sections for exotic actinide nuclei, Nucl. Sci. Eng. 72 (1979) 222.
[99] IGNATYUK, A.V., MASLOV, V.M. and PASHCHENKO, A.B., Coordinated analysis of the cross-sections for (n,f) and (n,Xn) reactions for actinides, Nucl. Phys. 47 (1988) 355-362 [in Russian].
[100] ASANO, N., MATSUNOBU, H., KIKUVHI, Y., Evaluation of neutron nuclear data for uranium-233, J. Nucl. Sci. and Techn. 19 (1982) 1037.

[101] KOBAYASHI, K., HASHIMOTO, T., KIMURA, I., Measurement of average cross-section for $^{233}U(n,2n)^{232}U$ reaction, J. Nucl. Sci. and Techn. 10 (1973) 668.
[102] CRANBERG, L., FRYE, G., NERESON, N., et al., Fission neutron spectrum of ^{235}U, Phys. Rev. 103 (1956) 662.
[103] KLEPATSKIJ, A.B., KON'SHIN, V.A., MASLOV, V.M., et al., Evaluated neutron constants for uranium-236, Preprint IYaEh-2, Minsk, Nuclear Power Institute of Acad. Sciences of Byelorussian SSR, 83 pp [in Russian].
[104] STAROSTOV, B.I., NEFEDOV, V.N. and BOJTSOV, A.A., Spectra of prompt neutrons from the fission of ^{233}U, ^{235}U and ^{239}Pu by thermal neutrons and from the spontaneous fission of ^{252}Cf in the 0.01-12 MeV energy range, in: Problems of Atomic Science and Technology, ser. Nuclear constants, No. 3 (1985) 16-24 [in Russian].
[105] SMITH, A.B., GUENTER, P., WINKLER, G., et al., Note on the prompt fission neutron spectra of uranium-233, -235 and plutonium 239 and -240 relative to that of californium-252, Nucl. Sci. eng. 76 (1980) 357.
[106] MADLAND, D.G., NiX, J.R., New calculation of prompt fission neutron spectra and average prompt neutron multiplicities, Nucl. Sci. Eng. 81 (1982) 213.
[107] HOWERTON, R.J., DOYAS, R.G., Fission temperatures as a function of the average number of neutrons from fission, Nucl. Sci. Eng. 46 (1971) 414.
[108] MANERO, F., KONSHIN, V.A., Status of the energy dependency of nu-bar values for the heavy isotopes (Z > 90) from thermal to 15 MeV and of nu-bar values for spontaneous fission, At. Energy Rev. 10 (1972) 637.
[109] MALINOVSKIJ, V.V., VOROB'EVA, V.G. and KUZ'MINOV, B.D., Review of the results of measurements of the average number of prompt fission neutrons, Problems of Atomic Science and Technology, ser. Nuclear constants, No. 5 (54) (1983) 19-56.
[110] GWIN, R., SPENSER, R.R., INGLE, R.W., Measurements of the energy dependence of prompt neutron emission from ^{235}U and ^{239}Pu for En = 0.0005 to 10 MeV relative to emission from spontaneous fission of ^{252}Cf, Nucl. Sci. Eng. 94 (1986) 365.
[111] BENEDETTI, G., CESANA, A., SANGIUST, V., et al., Delayed neutron yields from fission of uranium-233, neptunium-237, plutonium-238, -240, -241 and americium-241, Nucl. Sci. Eng. 80 (1982) 379.